Institut für Molekulare Mechanismen bei Krankheiten
der Vetsuisse-Fakultät Universität Zürich

Direktor: Prof. Dr. Dr. Michael O. Hottiger

Arbeit unter wissenschaftlicher Betreuung von Prof. Dr. Dr. Michael O. Hottiger

ARH1 regulates LPS-induced *iNOS* expression

Inaugural-Dissertation

zur Erlangung der Doktorwürde der
Vetsuisse-Fakultät Universität Zürich

vorgelegt von

Anne Marie Roentgen

Tierärztin
von Thalwil ZH

genehmigt auf Antrag von

Prof. Dr. Dr. Michael O. Hottiger, Referent
Prof. Dr. Hanspeter Nägeli, Korreferent

2017

Table of Contents

10 Acknowledgements

11 Curriculum vitae

1 Zusammenfassung

Protein-ADP-Ribosylierung ist eine reversible posttranslationelle Modifikation, die an Transkription, Proliferation und Apoptose, sowie an Entzündungskrankheiten und Krebs beteiligt ist. ADP-Ribosylhydrolase 1 (ARH1) entfernt mono-ADP-Ribose von Proteinen und zeigt eine tumorsuppressive Wirkung *in vivo*. Ein Effekt von ARH1 auf die Entzündungskaskade wurde bisher nicht gezeigt. Das Ziel der Studie war, einen funktionellen Einfluss von ARH1 auf die Lipopolysaccharid (LPS)-induzierte Entzündungskaskade zu überprüfen und den involvierten Mechanismus aufzuklären. Die siRNA-vermittelte Expressionsreduktion von ARH1 steigerte die LPS- oder LPS plus Interferon-gamma (IFNγ)-induzierte Genexpression der *induzierbaren Stickstoffmonoxid-Synthase* (*iNOS*) und des *IFNγ-induzierten Proteins 10* (*IP-10*) in NIH/3T3 Zellen. Die Überexpression von ARH1 Wildtyp oder einer enzymatisch inaktiven Mutante in siARH1 behandelten Zellen zeigte, dass der reprimierende Effekt von der ARH1 enzymatischen Aktivität abhängig ist. Zusätzlich wurden ADP-Ribosyltransferase 8 (ARTD8) und Signal transducer and activator of transcription 6 (Stat6) als Co-Regulatoren der LPS-induzierten *iNOS* Expression identifiziert. Die gleichzeitige Expressionsreduktion von ARTD8 oder Stat6 hob den reprimierenden Effekt von ARH1 auf die *iNOS* und *IP-10* Genexpression markant auf. Zusammenfassend zeigt diese Studie, dass die Aktivität von ARH1 die LPS-induzierte Entzündungskaskade via Interaktion mit Stat6 und ARTD8 reprimiert.

2 Summary

Protein-ADP-ribosylation is a reversible posttranslational modification (PTM) linked to transcription, proliferation as well as apoptosis, and contributes to inflammatory diseases and cancer. ADP-ribosylhydrolase 1 (ARH1) removes mono-ADP-ribose from proteins and has a suppressive effect on cancer development *in vivo*. However, an effect on inflammatory signaling has not been shown. The aim of the study was to elucidate the functional contribution of ARH1 in lipopolysaccharide (LPS)-induced pro-inflammatory signaling and the underlining molecular mechanisms.

siRNA-mediated knockdown of *ARH1* enhanced LPS- or LPS plus interferon gamma (IFNγ)-induced *inducible nitric oxide synthase* (*iNOS)* and *interferon gamma-induced protein 10* (*IP-10)* gene expression in NIH/3T3 cells. Overexpression of ARH1 wildtype and an enzymatically inactive mutant in siARH1 treated cells revealed that the repressory effect of ARH1 is dependent on its enzymatic activity. Furthermore, both ADP-ribosyltransferase 8 (ARTD8) and the signal transducer and activator of transcription 6 (Stat6) were identified as co-regulators of LPS-induced *iNOS* expression. Interestingly, concomitant knockdown of either ARTD8 or Stat6 with ARH1 markedly reversed the repressory effect of ARH1 on *iNOS* and *IP-10* expression. Thus, this study demonstrates that ARH1 activity represses LPS-induced *iNOS* expression via a crosstalk with Stat6 and ARTD8.

3 Abbreviations

A	Alanine
ADP	Adenosine diphosphate
ANK	Ankyrin repeat
ARH	ADP-ribosyl hydrolase
ARTC	ADP-ribosyltransferase clostridia toxin
ARTD	ADP-ribosyltransferase diphtheria toxin
BB	Binding Buffer
bp	Base pairs
CD-40	Cluster of differentiation 40
D	Aspartate
DNA	Deoxyribonucleic acid
dNTP	Deoxy Nucleotide-Tri-Phosphate
E	Glutamate
E. coli	*Escheria coli*
EB	Elution Buffer
eNOS	Endothelial nitric oxide synthase
EV	Empty vector
FL	Full length
Fr	Fragment
GFP	Green fluorescence protein
GST	Glutathione S-transferase
H_2O_2	Hydrogen peroxide
hARH	Human ARH
HDAC	Histone deacetylase
IFNγ	Interferon gamma
IKK	IκB kinase
iNOS	Inducible nitric oxidesynthase
IκB	NF-κB inhibitor
JAK	Janus kinase
K	Lysine
LPS	Lipopolysaccharide
LSD	Lysine specific demethylase
MAR	Mono-ADP-ribose
mARH	Murine ARH
MARylation	Mono-ADP-ribosylation
ml	Milliliter
mM	Millimolar
MS	Mass spectrometry
mut	Mutant
NAD^+	Nicotinamide adenina dinucleotide
NF-κB	Nuclear factor κB
ng	Nanogramm

NIK	NF-κB inducing kinase
nNOS	Neuronal nitric oxide synthase
NO	Nitric oxide
PAR	Poly-ADP-ribose
PARG	Poly(ADP-ribose) glycohydrolase
PARP	Poly(ADP-ribose) polymerase
PARylation	Poly-ADP-ribosylation
PBM	PAR-binding motif
PBS	Phosphate buffered saline
PBZ	PAR-binding zinc finger
PCR	Polymerase Chain Reaction
pH	Power of hydrogen
R	Arginine
RANK	Receptor activator of NF-κB
RHD	Rel homology domain
RNA	Ribonucleic acid
rpm	Rounds per minute
SDS-PAGE	Sodium dodecyl sulfate polyacrylamid gel electrophoresis
Stat	Signal transducer and activator of transcription
TAD	Transactivation domain
TBS	Tris buffered saline
TBS-T	Tris buffered saline Tween 20
TLR	Toll like receptor
TNFα	Tumor necrosis factor α
Tyr	Phosphotyrosine
WB	Washing buffer
wt	Wildtype
µl	Microliter
µM	Micromolar

4 Introduction

4.1 ADP-ribosylation

Protein ADP-ribosylation is a biochemically complex, reversible post-translational modification (PTM) conserved in all organisms from bacteria to humans, except in yeasts [1]. The PTM is initiated by a family of ADP-ribosyltransferases (ARTs) and a subclass of sirtuins, so called writers, transferring an ADP-ribose unit from nicotinamide adenine dinucleotide (NAD^+) to specific amino acid acceptor sites [2]. Readers containing specific binding moieties recognize distinct parts of the ADP-ribose. ADP-ribosylhydrolases remove the ADP-ribosylation PTM in consecutive steps and are thus erasers of this modification (Figure 1) [2-4].

There are two different types of protein ADP-ribosylation: mono-ADP-ribosylation (MARylation), when only one ADP-ribose is transferred to an acceptor amino acid of a target protein, or poly-ADP-ribosylation (PARylation), which involves the transfer and elongation of the initial protein bound ADP-ribose moiety to generate either linear or branched poly-ADP-ribose (PAR) chains [1, 5]. Quantitatively, MARylation, which is mainly synthesized extranuclearly, is more prevalent in cells than PARylation, which is predominantly found on nuclear proteins [6]. The half-life of protein PARylation is shorter than that of MARylation [7].

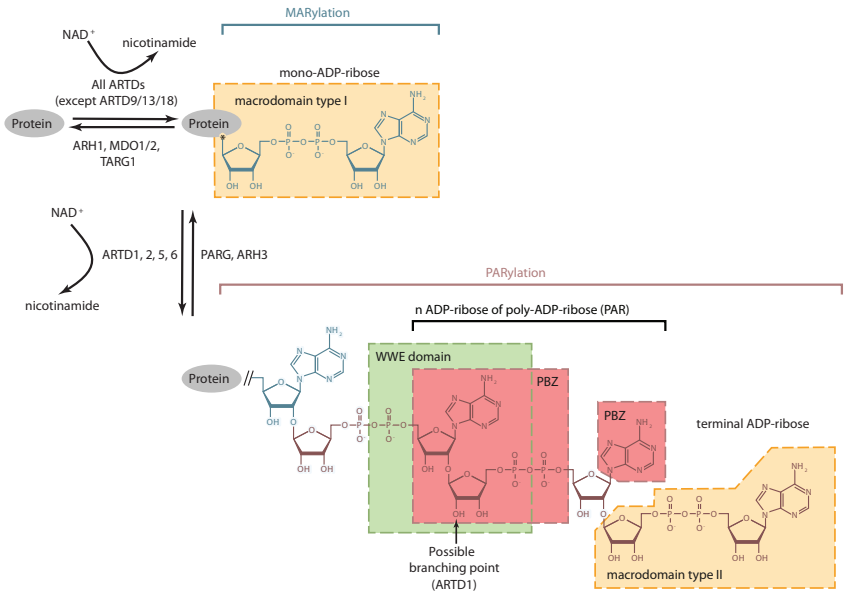

Figure 1: Schematic view on ADP-ribosylation.

ADP-ribosylation can be detected in different ways. First, ADP-ribosylated proteins can be modified and detected *in vitro* by using radiolabeled NAD^+. However, it is more difficult to detect ADP-ribosylated proteins *in vivo* [8]. The very short half-life of protein ADP-ribosylation makes the latter difficult to detect in general. Although antibodies can detect PARylation, there are no antibodies that can detect MARylation. Antibodies against PARylation are usually used for immunofluorescence and immunoblotting.

4.1.1 Writers

ARTs are divided into two subclasses according to their structure, namely into diphtheria toxin-like ARTs (ARTDs) and cholera toxin-like ARTs (ARTCs) [1]. The human ARTC family consists of 5 members. In contrast to the ARTDs, which are localized intracellularly, ARTCs are localized at the cell membrane in direction to the extracellular space [1]. The ARTD family is characterized by the presence of the PARP catalytic domain that catalyzes the transfer of ADP-ribose moieties from NAD^+ to acceptor proteins. From the 18 human ARTD members, ARTD3, ARTD4, ARTD7-8, ARTD10-12 and ARTD14-17 catalyze MARylation, whereas ARTD1, ARTD2, ARTD5 and ARTD6 catalyze PARylation by attaching more than one ADP-ribose to the protein or the protein-bound ADP-ribose unit (Table 1). PARylation results in linear or branched poly-ADP-ribose (PAR) chains [9].

Name	Alternative Names	Enzymatic Activity (automodification)	Cellular Localization[1]
ARTD1	PARP1	PARylation, branching	N
ARTD2	PARP2	PARylation	N >> C
ARTD3	PARP3	MARylation	N > C
ARTD4	PARP4, vPARP	MARylation	C > N
ARTD5	PARP5A, tankyrase 1	OARylation	C >> N
ARTD6	PARP5A, PARP6, tankyrase 2	OARylation	C >> N
ARTD7	PARP15, BAL3	MARylation	C
ARTD8	PARP14, BAL2, CoaSt6	MARylation	C > N
ARTD9	PARP9, BAL1	no activity reported	C >> N
ARTD10	PARP10	MARylation	C >> N
ARTD11	PARP11	MARylation	N and C
ARTD12	PARP12, ZC3HDC1	MARylation	C >> N
ARTD13	PARP13, ZC3HAV1, ZAP1	no activity reported	C
ARTD14	PARP7, tiPARP, RM1	MARylation	C and N
ARTD15	PARP16	MARylation	C
ARTD16	PARP8	MARylation	C
ARTD17	PARP6	MARylation	C
ARTD18	TPT1	no activity reported	unknown

Table 1: Localization and enzymatic activity of mono- and poly-ARTDs [2]

In humans, in addition to the ARTDs, also SIRT family members were described to MARylate proteins. The SIRT family contains seven members. The seven members are located in different cellular compartments and have different enzymatic activities. SIRT4 and SIRT6 have NAD^+-dependent mono-ART activity [10].

Writers transfer ADP-ribose to different acceptor sites [11]. Mammalian ARTDs seem to modify preferentially lysines, glutamic acids, aspartic acids or lysines. Additionally, ADP-ribosylation on cysteines, dipthamides and phosphoserines has been described [1, 12, 13]. In contrast to ARTDs, mammalian ARTCs are specific for arginines as acceptor residues [14].

4.1.2 Readers

Protein ADP-ribosylation allows the recruitment of other proteins. These proteins, also called readers, contain protein domains that non-covalently bind to ADP-ribosylated proteins. Four distinct classes of binding domains are known to exert this reader function: WWE domains, macrodomains, PAR-binding motifs (PBMs) and PAR-binding zinc-fingers (PBZs). There are many human proteins, including some ARTDs, e.g. ARTD8, that contain such protein domains [1].

4.1.3 Erasers

ADP-ribosylhydrolases are enzymes that reverse MAR- and PARylation. To date, three classes of these enzymes have been described: The poly-ADP-ribosyl glycohydrolase (PARG) isoforms, ADP-ribosylhydrolases (ARHs) and the macrodomains (MDOs). PARG was the first enzyme shown to have a poly-ADP-ribosylhydrolase activity, but has no activity towards the terminal protein-bound ADP-ribose. A similar PARG activity was proposed for the structurally unrelated ADP-ribosylhydrolase 3 (ARH3), which is only known to release PAR. ADP-ribosylhydrolase 1 (ARH1) was the first hydrolase shown to reverse mono-ADP-ribosylation, but only from arginines. MDO1, MDO2 and C6orf130 were identified to release the terminal single ADP-ribose from the amino acids glutamic acid or aspartic acid. To date, ADP-ribosylation is known to be fully reversible from all identified ADP-ribose acceptor amino acids, except from lysines [1, 15, 16].

4.2 The ARH family

The ARH family consists of 3 family members: ARH1, ARH2 and ARH3. The family members have a similar size (about 39 kDa) and amino acid sequence (Figure 2) [4]. The amino acid sequences of human ARH1 and ARH2 are 45–47% identical to one another, but only about 22% identical to that of ARH3 [1].

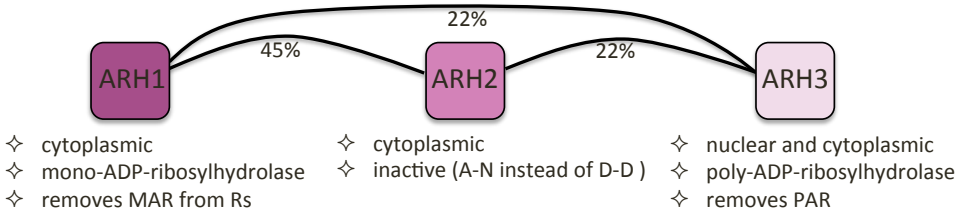

Figure 2: Charakterization of the ARH family members [1]

While ARH2 is only expressed in heart myocytes, sceletal myocytes, brown fat and non-lactating mammary glands, ARH1 and ARH3 are expressed in many different tissues (www.biogps.org). ARH1 was reported to be a cytoplasmic protein, whereas ARH3 is localized in the nucleus as well [1]. ARH2 is known to be localized in the cytoplasm [17].

Together with PARG and the MDOs, ARH1 and ARH3 are responsible for the removal of intracellular protein ADP-ribosylation. The enzymatic activities of ARH1 and ARH3 require Mg^{2+} and can be inhibited by ADP-ribose [4]. ARH1 and ARH3 possess vicinal acidic amino acids, two aspartic acids, at position 77/78 for human ARH3 and at position 60/61 for human ARH1, that allow coordination of Mg^{2+}. Replacement of these two aspartic acids by asparagine or alanine renders ARH1 and ARH3 inactive. ARH2 contains an asparagine and alanine instead of two aspartic acids at this position. This could be the reason why ARH2 is inactive and not able to hydrolyze ADP-ribose [15].

ARH1 is a 39 kDa mono-ADP-ribosylhydrolase that hydrolyzes the N-glycosidic bond of a mono-ADP-ribose attached to arginines. Moreover, it possesses weak hydrolytic activity towards the O-glycosidic bond of PAR and OAADPr. In contrast, ARH3 has poly-ADP-ribosylhydrolase activity that cleaves the only O-glycosidic bond in PAR and OAADPr [15].

4.3 Function of protein ADP-ribosylation

ADP-ribosylation of proteins regulates cellular functions by different mechanisms [9]. Two examples are DNA repair proteins that bind to PAR, which is necessary for their recruitment to damaged DNA and ADP-ribosylation of proteins that influence protein/protein or protein/DNA interactions. ADP-ribosylation thus participates in a wide range of cellular processes such as the DNA damage response, transcription, cell proliferation or cell death (Figure 3) [18, 19].

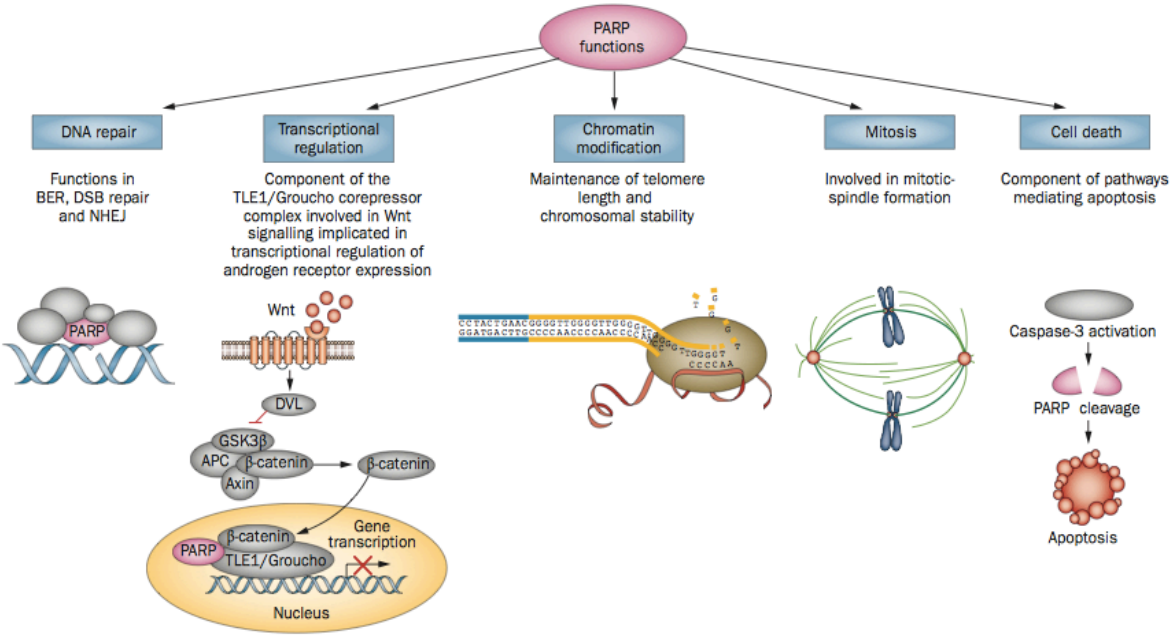

Figure 3: Cellular functions of the ARTD family members [20]

At the tissue or at the organismal level, ADP-ribosylation has been described to be associated particularly with inflammation and cancer formation [12]. If cells are stressed by DNA lesion-inducing agents, several signaling pathways are initiated resulting in the activation of e.g. ARTD1 or ARTD2 [21]. ARTD1, ARTD2 and PARG are involved in the genotoxic stress response to favor DNA repair [22]. This indicates that ARTDs help cells, also cancer cells, to survive and enhance tumor formation and progression.

PARylation is involved in many basic processes such as DNA replication, repair and transcription [23]. During inflammation, ARTD1 was shown to activate the nuclear factor kappa-light-chain-enhancer of activated B cells (NF-κB) pathway, the nuclear factor of activated T-cells (NF-AT) pathway and to boost in this way the expression of different cytokines, e.g. *tumor necrosis factor alpha* (*TNFα*), *interferon gamma* (*IFNγ*), and

interleukin 6 (*IL-6*), *inducible nitric oxide synthase* (*iNOS*), chemokines and other inflammatory proteins [24, 25].

MARylation has also been linked to several diseases, such as inflammatory diseases and cancer [26]. ARTD10 has been reported to be involved in inflammation. It MARylates NF-κB essential modulator (NEMO) and reduces poly-ubiquitination, which leads to an increased stability of NF-κB inhibitor (IκB) and therefore a reduced p65 nuclear translocation and gene expression [27]. Additionally, ARTDs involved in MAR formation have been shown to modulate cell survival and apoptosis [26]. ARTD9, a catalytically inactive ARTD [28], has been described to act as an oncogenic factor in diffuse large B-cell lymphoma [29], by modulating IFNγ-Stat1 signaling to repress tumor suppressor genes and activate proto-oncogenes [29].

Until now, several pharmacological inhibitor s against ARTDs were shown to reduce symptoms or the susceptibility of certain diseases. For instance, ARTD inhibitors have protective effects in acute and chronic inflammatory diseases such as rheumatoid arthritis, colitis and allergies [24, 30].

Also, ADP-ribose erasers have been reported to regulate tumorigenesis and inflammation. For instance, tumor cells (e.g. lymphomas, adenocarcinomas) injected in ARH1-deficient mice developed into tumors, while those injected into ARH1-proficient mice did not as frequently [31]. In another *in vivo* experiment, ARH1-deficient tumor cells developed into tumors when injected in nude mice, while nude mice injected with ARH1-proficient tumor cells did not, indicating that ARH1 may be involved in cancer repression [32].

The current lack of tools to analyze and investigate PAR- and MARylation raises the possibility that these modifications have been largely underestimated compared with other PTMs [12]. Together, ADP-ribosylation is an interesting PTM that is involved in many physiological processes. For the future, it would be interesting to understand all these functions and to elucidate the influence of ADP-ribosylation on different diseases.

4.3.1 The transcription factor Nuclear Factor kappa B (NF-κB)

NF-κB is a transcription factor family that plays an important role in the cellular pro-inflammatory response. The family consists of 5 related family members including RelA, RelB, c-Rel, p105/p50 and p100/p52. All family members bind to DNA in a variety of

heterodimeric and homodimeric complexes and are operating in two different NF-κB pathways that are activated by different stimuli: the canonical/classical and the non-canonical/alternative pathway (Figure 5) [33].

The NF-κB family members all share a highly conserved amino-terminal rel homology domain (RHD), which is important for the dimerization, nuclear translocation, DNA binding and interaction with the inhibitory IκB proteins. RelA, RelB, and c-Rel additionally possess a carboxy-terminal transactivation domain (TAD) that initiates transcription of NF-κB target genes. The ankyrin (ANK)-containing precursor proteins p105 and p100 are proteolytically processed to p50 and p52 upon cellular stimulation (Figure 4) [34]. Upon pro-inflammatory stimulation, NF-κB complexes translocate to the nucleus and bind to promoter or enhancer regions of NF-κB target genes [35].

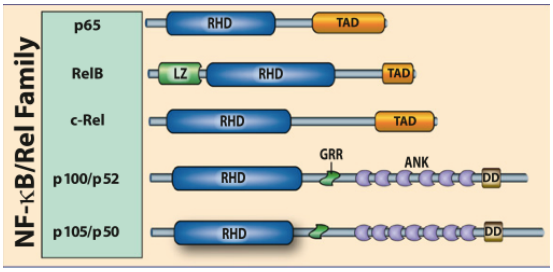

Figure 4: Structural components of the NF-κB family [36]

NF-κB family members regulate the gene expression of several cytokines (e.g. *IL-6, IP-10, IFNγ, COX-2*) growth factors (e.g. *G-CSF, iGFBP-2*), transcription factors (e.g. *IκBα, c-Rel, IRF-1*) and inhibitors of apoptosis (e.g. *Bcl-xL, Fas-Ligand*) and are therefore involved in many cellular processes like inflammation, cell proliferation and apoptosis [37].

4.3.2 The canonical NF-κB pathway

RelA (p65) and p50 are mainly involved in the canonical NF-κB pathway (Figure 5). These two NF-κB family members are expressed in almost every cell type and are localized in the cytoplasm and bound to an inhibitory IκB protein under unstimulated conditions. This pathway is activated by a variety of stimuli, such as LPS, TNFα or IL-1 through their cognate receptors (TLR4, TNFα, IL-1R). Upon activation of the signaling cascade, IκB gets phosphorylated, ubiquitinated and consequently degraded. This degradation of IκB leads to a release of RelA/p50 and a translocation of the RelA/p50 dimer into the nucleus. In the

nucleus, the dimer binds to DNA and activates transcription of its target genes, including genes encoding for members of the Rel/ NF-κB/IκB families [35, 38].

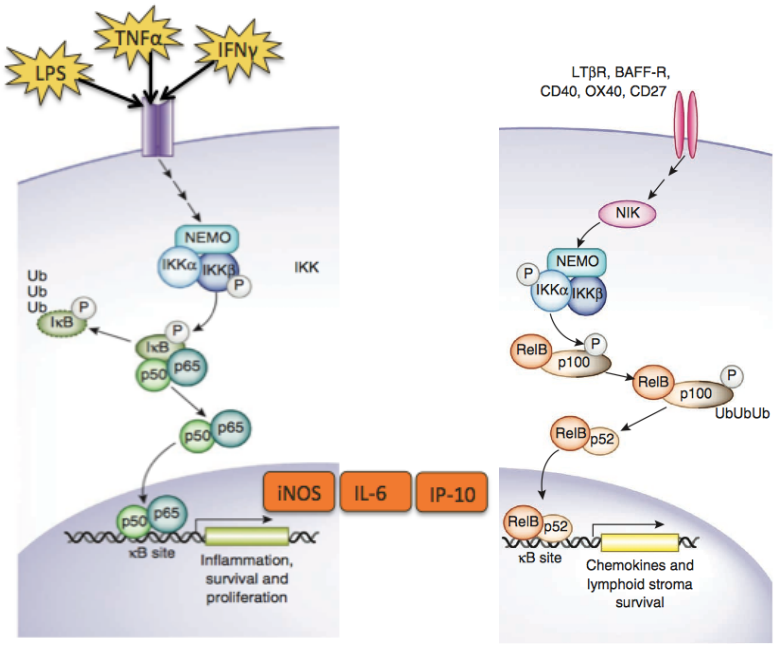

Figure 5: Canonical and non-canonical pathway of NF-κB [39]

Upon expression of particularly *IκB*, NF-κB limits its own activation. IκB enters the nucleus and interferes with the binding of NF-κB to DNA [35, 38].

4.3.3 The non-canonical NF-κB pathway

The non-canonical pathway of NF-κB is linked to activation of p52 and RelB (Figure 5). In this pathway, ligand induced activation of receptors (e.g. BAFFR, CD40, LTβR, RANK) results in the activation of NIK, which phosphorylates and activates the IKKα complex. The IKKα complex phosphorylates p100, leading to the processing and liberation of the p52/RelB active heterodimer. This p52/RelB heterodimer subsequently translocates to the nucleus and acts as transcription factor [34, 40].

4.3.4 Biological relevance of NF-κB induction

NF-κB is a key regulator of the pro-inflammatory response. NF-κB controls pro-inflammatory genes e.g. *iNOS, IP-10, IL-6*, but also genes that control cell proliferation and cell survival through expression of anti-apoptotic genes. Thus, it is very important to tightly

control the expression of NF-κB target genes, since overexpression often leads to inflammation-associated disorders, such as e.g. inflammatory bowel disease [41], arthritis [42] and asthma [43] or cancer development [44].

4.4 The signal transducer and activator of transcription (Stat) family

The signal transducer and activator of transcription (Stat) family consists of seven transcription factors. The seven members are especially activated by different growth factors and cytokines (Table 2). Once activated, Stat family members localize to the cytoplasm.

Molecule	"Inflammatory" activators	"Anti-inflammatory" activators	Heterodimerization partners
STAT1	Type I IFN Type II IFN IL-6	IL-10 IL-27 IL-35	STAT2 (IFN) STAT3 (IL-6, -27) STAT4 (IL-35)
STAT2	Type I IFN		STAT1 (IFN)
STAT3	IL-2 IL-5 IL-6 IL-23 MCSF GCSF	IL-10 IL-27	STAT1 STAT5a/b
STAT4	IL-12 IL-23	IL-35	STAT1 (IL-35) STAT3 (IL-23)
STAT5a/5b	IL-2 -7 -15 IL-21 M-CSF GM-CSF		STAT3 (IL-2, -7, GCSF, MCSF)
STAT6	Type I IFN (B and human T cells) IL-3 IL-4 IL-13		STAT2 (IFN) (B and human T cells)

Table 2: Stat family members and their activators [45]

The Stat family members are structurally composed of a conserved tyrosine residue near the C-terminus that is phosphorylated by Janus Kinases (JAKs). This phosphotyrosine (Tyr) regulates the dimerization of two Stats through interaction with a conserved SH2 domain of the second interacting Stat (Figure 6). Dimerization allows Stat family members to enter the nucleus [46, 47].

Figure 6: General structure of Stats (Coiled-coil (CC), DNA binding site (DBS)) **[46]**

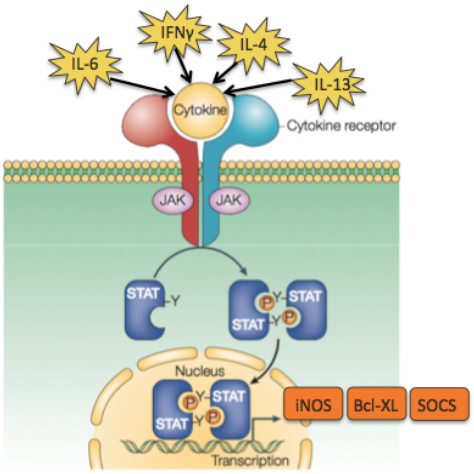

Figure 7: Schematic representation of the JAK-STAT signaling [48]

Through this dimerization and translocation to the nucleus, Stats deliver the signal from the cell surface to the nucleus as second messengers. In the nucleus, Stat dimers bind to DNA at their promoter regions and enhance gene transcription (Figure 7) [46, 47].

4.4.1 Stat6

Stat6 is a signaling molecule and acts as a transcription factor. In the nucleus Stat6 is also known to interact with p100 and NF-κB. The activation of Stat6 is initiated by IL-4 and IL-13 binding to their receptors. Binding to the receptor leads to an activation of JAK. The JAK itself and three tyrosine residues of the receptor become phosphorylated which allows Stat6 binding to the receptor and subsequent phosphorylation by JAK. Upon phosphorylation, Stat6 forms homodimers. This dimerization allows the nuclear translocation of Stat6 [47].

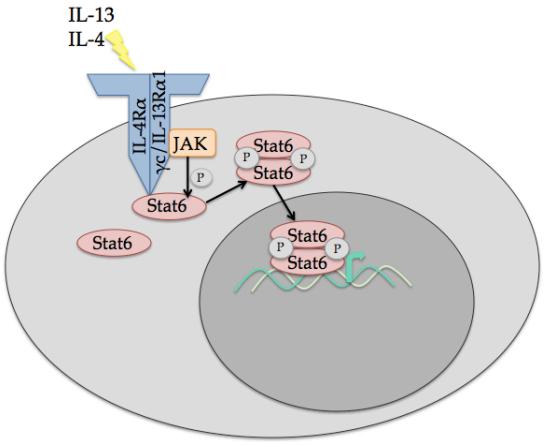

8: Scheme of activated Stat6 signaling

In the nucleus, Stat6 dimers bind to DNA and activate the transcription of their target genes (e.g. *TNF, IRF1, CCLII, ADAM8*) (Figure 8) [49]. Stat6 by itself needs regulatory co-factors like p100, NCoA-1, CoaSt6 and CREB-binding protein, to activate gene transcription efficiently. p100 enhances Stat6-dependent transcription by linking Stat6 to the RNA-polymerase II. In addition to its function as transcription factor, Stat6 induces the enzymatic activity of ARTD8 (formerly PARP-14) [47].

4.4.2 ARTD8 – a co-regulator of Stat6 induced gene expression

ARTD8 is a member of the ARTD superfamily localized in the cytoplasm and the nucleus. In addition to the catalytic domain, ARTD8 contains a macrodomain. ARTD8 is therefore able to MARylate proteins and to read and bind ADP-ribosylated proteins [50].

ARTD8 was described to regulate IL-4 dependent gene transcription. Under unstimulated conditions, ARTD8 forms a complex with Histone deacetylase (HDAC) 2 and 3 that is bound to Stat6-responding promoters. In the presence of IL-4 and activated Stat6, the enzymatic activity of ARTD8 is induced and ARTD8 converts into an activator. The catalytic domain of ARTD8 uses NAD^+ to MARylate itself, p100 and HDAC2 and 3. ARTD8 and the other factors consequently dissociate from the promoter and allow transcriptional co-activators like p300/CBP, NCoA-1 and NCoA-3 to be recruited to the promoters of Stat6 target genes and to acetylated histones, which leads to a relaxed chromatin structure. ARTD8 therefore enhances Stat6-dependent transcription by strengthening the binding of Stat6 to its promoters [50].

4.4.3 Biological relevance of Stat6

Stat6 is expressed in many cell types and plays an important role in the differentiation of Th2-cells and the B-cell induced expression of IgG and IgE. Additionally, it impairs cell proliferation, cell growth and apoptosis [50].

Stat6-dependent signaling plays a critical role for the late effector phase of airway responsiveness, including airway hyperresponsiveness, eosinophilia and mucus hypersecretion. Additionally, Th2 cell differentitation and Th2 response is dependent on Stat6 [51, 52]. STAT6 is important for allergic responses [53]. Also, a role of Stat6 in different carcinomas has been reported [54].

4.5 Nitric oxide synthase (NOS)

Nitric oxide synthase (NOS) is a family of enzymes that catalyze the conversion of L-arginine to L-citrulline and nitric oxide (NO). NO is an important cellular signaling molecule that acts as a biological mediator. It regulates blood vessel tone in vascular systems and is an important host defense effector in the immune system [55]. In humans, there are three isoforms of NOS known: inducible NOS (iNOS), endothelial NOS (eNOS) and neuronal NOS (nNOS). The three different isoforms are associated with different characteristics and gene expression patterns that define their nomenclature [56]. *eNOS* and *nNOS* isoforms are constantly expressed in resting cells and are therefore designated as constitutive NOS [55]. eNOS and nNOS are mainly found in non-immunological cells and are responsible for the NO production that mediates vascular homeostasis and intracellular signaling processes [56].

4.5.1 iNOS

iNOS is particularly induced in cells of the immune system and is necessary for the microbicidal activity of macrophages. Under unstimulated conditions, *iNOS* is expressed at very low levels and is undetectable in macrophages. Newly synthesized NO promotes inflammation and is cytotoxic. In contrast to eNOS and nNOS, iNOS functions in a calcium-independent manner and has a high affinity binding site for calmodulin [55]. *iNOS* expression depends on several factors, for instance intra- and extracellular stimuli and can differ between different species and even between different cell types of the same species. Upon a proinflammatory immunresponsive stimulation, like NF-κB, IFNγ and IL-4, *iNOS* expression is strongly induced. NF-κB directly binds to the iNOS promoter to activate *iNOS* transcription. IFNγ mediated *iNOS* expression can be dramatically increased by TNFα. Interestingly, TNFα alone has no influence on *iNOS* expression. The detailed molecular mechanisms how NF-κB and IFNγ activate *iNOS* expression is still unclear [56-58].

5 Aim of the thesis

Protein-ADP-ribosylation is a reversible PTM [1]. ADP-ribose is transferred from NAD^+ to an acceptor amino acid (e.g. glutamic acid, aspartic acid, arginine and lysine) of a target protein and onto protein-bound ADP-ribose itself by writers (ART's and sirtuins). ADP-ribosylation is sensed by protein readers that contain binding modules (PBM, PBZ domains, WWE domains, and macrodomains) recognizing specific parts of ADP-ribosylation [1]. There are three classes of erasers that reverse MAR- and PARylation: The PARG isoforms, the ARH family and the macrodomains [15].

While ARTDs and PARylation have been subject of various studies, comparably little is known about the ADP-ribosylhydrolases and MARylation [1]. The fact that some ARTD members are known to be involved in inflammation and catalyze the formation of MAR, points at an interesting potential role of mono-ADP-ribosylhydrolases in this condition. Therefore, it is not surprising that also MARylation and ADP-ribosylhydrolases have been linked to several diseases [12].

We thus hypothesized that ARH1 is a potential regulator of pro-inflammatory signaling. The aims of this thesis were therefore:

1. To elucidate a possible functional contribution of ARH1 on NF-κB-induced pro-inflammatory signaling.
2. To investigate the molecular mechanisms through which ARH1 potentially interferes with inflammatory signaling.

6 Material and Methods

6.1 Materials

6.1.1 Antibodies

1st antibodies

Antibody name	Manufacturer	Catalog number	Dilution WB	Dilution IF
Mouse monoclonal Anti-Flag (M2)	Sigma	F3165	1:1'000	1:1'000
Mouse monoclonal Anti-HA.11	Covance	MMS-101R	1:250	1:250
Mouse monoclonal Anti-α-Tubulin (DM1A)	Sigma	T6119	1:10'0000	-
Rabbit polyclonal Anti-GAPDH (FL-335)	Santa-Cruz	sc-25778	1:1'000	-
Rabbit polyclonal Anti-HMGB1	Abcam	ab18256	1:1'000	-
Rabbit polyclonal Anti-NFκB p65 (C-20)	Santa-Cruz	sc-372	1:1'000	1:250
Rabbit polyclonal Anti-PARP-1 (H-250)	Santa-Cruz	sc-7150	1:1'000	-
Rabbit polyclonal Anti-Stat6 (M-20)	Santa-Cruz	sc-981	1:500	1:250

2nd antibodies

Antibody name	Manufacturer	Catalog number	Dilution WB	Dilution IF
Polyclonal Cy™ 3 AffiniPure Goat Anti-Mouse IgG (H+L)	Jackson ImmunoResearch	115-165-146	-	1:250
Polyclonal Cy™ 3 AffiniPure Goat Anti-Rabbit IgG (H+L)	Jackson ImmunoResearch	111-165-003	-	1:250
Polyclonal IRDye 800CW Goat anti-Mouse IgG (H+L)	Li-Cor	926-32210	1:15'000	-
Polyclonal IRDye 680 (red) Goat anti-Rabbit IgG (H+L)	Li-Cor	926-68071	1:15'000	-

Table 3: Antibodies used for immunoblot and immunofluorescence

6.1.2 Primers for cloning

All primers were ordered from Microsynth.

OTM	Primer name	5'-sequence
2230	hARH1_for	GCAGGATCCATGGAGAAGTATGTGG
2231	hARH1_rev	CGGCTCGAGCTAAAGGGAAATTACAGT
2240	hARH1_D60/61A_for	GAGAGTTAGTGCCGCCACAGTGATGC
2241	hARH1_D60/61A_rev	GCATCACTGTGGCGGCACTAACTCTC
2448	XhoI_mARH1_f	GCACTCGAGTGATGGGTGGGGGGCTGA
2449	BamHI_mARH1_r	GCAGGATCCCTAGGGATCTAATACAGGGTC
2450	XhoI_hARH1_f	GCACTCGAGTGATGGAGAAGTATGTGG
2451	BamHI_hARH1_r	GCAGGATCCCTAAAGGGAAATTACAGT
2452	BamHI_mARH1_f	GCAGGATCCATGGGTGGGGGGCTGATT
2453	XhoI_mARH1_r	GCACTCGAGCTAGGGATCTAATACAGGGTC
2454	mARH1 D61/62A for	GAGAGTCAGTGCTGCTACCGTCATGC
2455	mARH1 D61/62A rev	GCATGACGGTAGCAGCACTGACTCTC
2550	EcoRI_mARH1_rev	GCAGAATTCCTAGGGATCTAATACAGGGTC

Table 4: Primers used for cloning

6.1.3 Primers for quantitative real-time polymerase chain reaction (qRT-PCR)

All primers were ordered from Microsynth.

OTM	Primer Name	5'-Sequence
358	mouse rps12 for	GAAGCTGCCAAAGCCTTAGA
359	mouse rps12 rev	AACTGCAACCAACCACCTTC
368	mIL6-F	CCAATTTCCAATGCTCTCCT
369	mIL6-R	ACCACAGTGAGGAATGTCCA
460	mIkBa-Fw	AAATCTCCAGATGCTACCCGAGAG
461	mIkBa-Rev	ATAATGTCAGACGCTGGCCTCCAA
687	mIp10-F	GTCTGAGTGGGACTCAAGGGATC
688	mIp10-R	CACTGGCCCGTCATCGATAT
691	hIL-6-F	GGCACTGGCAGAAAACAACC
692	hIL-6-R	GCAAGTCTCCTCATTGAATCC
693	hGAPDH-F	TGCACCACCAACTGCTTAGC
694	hGAPDH-R	GGCATGGACTGTGGTCATGAG
753	HINOS-F	ATGAGGACCACATCTACC
754	INOS-R	CCTGAACATAGACCTTGG
1021	1021_mTNFA_F	ACGGCATGGATCTCAAAGAC
1022	1022_mTNFA_R	AGATAGCAAATCGGCTGACG
1111	mRelA F	GCGAGACCTGGAGCAAGCCATT
1112	mRelA_R	GTGTTGGGGGCCCGGTTATCAA
1461	mRelB_fwd	GGCTTTGGCCTGGACGGGAC
1462	mRelB_rev	CTCGAAGCTCGATGGCGGGC
2065	mARTD8_qPCR_fwd	AAGAACGCTACTGCCTACGG
2066	mARTD8_qPCR_rev	TATGTGCGGGTTCTCACTGG
2267	hADPRH(ARH1)_for	TTCAACACTGGTCCTACTTCCAAACC
2268	hADPRH(ARH1)_rev	CTTCCAGGAGTCTCCTGCAGCAA
2269	mAdprh(Arh1)_for	CTTCAACACTGGTCCTACTTCGAGA
2270	mAdprh(Arh1)_rev	ACCCCAGCCCGAGTAGCTCA
2273	mAdprhl1_for	CCCTGACCACAGACTACTGGTG
2274	mAdprhl1_rev	GCAGCTCCGAATCCTGAACCCTT
2277	miNOS_f	AGTCAACTGCAAGAGAACGGA
2278	miNOS_r	TGAGAACAGCACAAGGGGTT
2433	mArh2_fwd	CTCCCAGCTGAAACCGGATA
2434	mArh2_rev	AGGGACCCAAGGAAACCTGTA
2589	mSTAT6for	CCTGGTCGGTTCAGATGCTT
2590	mSTAT6rev	CAGGTGGCGGAACTCTTCTA

Table 5: Primers used for qPCR

6.1.4 siRNAs

All siRNAs were ordered from Qiagen

Gene	siRNA name	Sequence	Product ID
ARH1	Mm_Adprh_6	CAGAAACCTCATAACCTTGTA	SI04390323
ARH2	Mm_Adprhl1_1	CCGAGAGATGGTAAAGCGCTA	SI00890575
ARTD8	Mm_Parp14_8	CAAGAGCATTCGATTGGCTAA	SI02846669
Mock	Allstars neg. control	unknown	SI03650318
RelA	Mm_Rela_2	ATGGAGTACCCTGAAGCTATA	SI01399622
Stat6	Mm_Stat6_4	CCAGAAGATCTTCAACGACAA	SI00183596

Table 6: siRNAs used for transfection

6.1.5 Stimuli

Stimulus	Species	Manufacturer	Used Concentration
H_2O_2	Not applicable	Sigma	1 mM
LPS	*E. coli* 055:B5	Sigma	100 ng/ml
IFNγ	Mouse	BioVision	10 ng/ml

Table 7: Stimuli used for cell treatment

6.2 Cell culture methods

6.2.1 Cultivation

Aliquots of frozen NIH3T3 cells (obtained from Jeannette Abplanalp, DMMD UZH), HEK293 cells (obtained from Friedrich Kunze, DMMD UZH) or HEK TLR4 cells (obtained from Ann-Katrin Hopp, DMMD UZH) were thawed at 37°C in a water bath for 5 min and centrifuged for 3 min at 1970 rcf. Then, the cells were resuspended in fresh DMEM (Gibco by life technologies) containing 1% penicillin/streptomycin and 10% fetal calf serum and cultivated at 37°C in a CO_2 incubator. Cells were split at a confluence of 90-100%. Thereafter, cells were first washed twice with 3 ml of 1x phosphate buffered saline (PBS, 0.1 M, pH 7.4) (for a 10 cm dish), then detached with 1 ml trypsin (for a 10 cm dish) followed by an incubation at 37°C for 2 min. After these 2 min, 1 ml of DMEM was added to the cells and 5% of the cells were transferred to a new plate (10 cm dish) containing 10 ml fresh DMEM. Cells were counted in a Neubauer chamber by adding cell solution mixed with trypan blue at a ratio of 1:1. The required number of cells was seeded onto new plates and incubated again at 37°C.

6.2.2 siRNA cell transfection

Cells were transfected with siRNA using Lipofectamine® RNAiMAX Reagent (invitrogen by life technologies). First, NIH3T3 cells were grown in six well dishes to a confluence of 60-80% at the time of transfection. The transfection solution was prepared according to the manufacturer's protocol (500 μl Opti-MEM® (Gibco by life technologies), 3 μl of siRNA (Table 6) (1 μg/μl) and 3 μl Lipofectamine for a each well of a 6 well dish) and incubated at room temperature (RT) for 20 min. Then, the siRNA-lipid complex was added to cells by swirling the plate and together incubated for 48 h at 37°C. The transfected cells were used for whole cell extracts, cytosolic extracts and for RNA isolation to check gene expression.

6.2.3 Plasmid DNA cell transfection

Cells were split into 24 well or 15 cm dishes so that they reach a confluence of 40% at the day of transfection. Then, the transfection reagent was prepared: 2x BES (50 mM BES, 280 mM NaCl, 0.594 mM Na_2HPO_4 in ddH_2O) was thawed and brought to RT and 2.5 M $CaCl_2$ was prewarmed to 37°C. For a cell culture in 500 μl DMEM, 21.9 μl ddH_2O with 3 μl 2.5 M $CaCl_2$ and 0.5 μg of the plasmid DNA was first mixed. Then, 25 μl 2x BES was added dropwise to the DNA/$CaCl_2$ mixture and incubated for 3 min at RT. After the incubation, the transfection mix was immediately dropped onto the well without swirling and cells incubated at 37°C for 6 h. After 6 h, the cells were washed once with 250 μl 1x PBS and resuspended in 500 μl fresh DMEM. The cells were used for immunofluorescence and cellular extracts after 48 h and for RNA isolation after 24 h.

6.2.4 Cell treatment

3T3 and HEK TLR4 cells were treated with different stimuli (Table 7) to activate NFκ-B-dependent signaling or to activate an oxidative stress response. Before adding the respective stimulus to the cells, the medium was changed. LPS was added and incubated for 1 h or 4 h at a concentration of 100 ng/ml medium and IFNγ at a concentration of 10 ng/ml medium for gene expression analysis. For immunofluorescence, the cells were stimulated with LPS at a concentration of 100 ng/ml medium for 30 min and 1 mM H_2O_2 for 10 min.

6.2.5 Immunofluorescence

First, a round cover slip was added to each well of 24 well dishes. Then, NIH3T3 cells or HEK TLR 4 cells were seeded and transfected with plasmid DNA 1 d later and incubated for 48 h, so that they finally reached a confluence of 70% before analysis by immunofluorescence. The cells, untreated or treated with LPS, were first fixed with 300 μl of 4% paraformaldehyde in PBS (PFA) and incubated for 15 min on a shaker at RT. Then the PFA was removed and 500 μl of 0.2% Triton X-100 in 1x PBS was added to the cells and incubated on a shaker for 10 min at RT. After incubation with 0.2% Triton X-100, the slides were washed twice with 300 μl 1x PBS and blocked with 300 μl blocking solution (2% BSA, 0.1% Triton X-100 in 1x PBS) for 45 min at RT. Then, the first antibody (Table 3) was freshly prepared in blocking solution and 25 μl of the first antibody dropped onto each slide placed on a parafilm. The slide was then laid upside down on this antibody drop. The slides were washed twice with 300 μl PBS after 1 h incubation with the first antibody to reduce unspecific binding. The procedure for the second antibody was the same as for the first antibody, except that the incubation time was only 45 min and everything was done in the dark. The slides were then once washed with 1x PBS and laid upside down on a microscope slide with a drop of VECTASHIELD® mounting medium containing DAPI (Vector Laboratories) and after drying, fixed with nail polish.

Cells, treated with H_2O_2 were fixed for 5 min on ice with freshly prepared methanol/acetic acid (3:1, v/v). Then the cells were washed twice with 1x PBS at RT and blocked for 30 min with 100 μl PBSMT (5% milk, 0.05% Tween 20 in 1x PBS). The cells were incubated for 1 h at RT with 25 μl of the first antibody (see materials) with coverslips placed upside down on parafilm. After 1 h of incubation, the slides were washed twice for 20 min with 300 μl PBS. The cells were then incubated for 1 h protected from light with the second antibody (Table 3). The slides were washed again for 25 min with 1x PBS and then laid upside down on a microscope slide with a drop of VECTASHIELD® mounting medium containing DAPI and fixed with nail polish.

The samples were stored at 4°C protected from light and analyzed by fluorescence microscopy. After a short general inspection to evaluate the transfection rate, the cells were analyzed under fluorescent light and pictures were taken.

6.3 Nucleic acid-based methods

6.3.1 RNA purification

RNA was isolated from cells with the NucleoSpin® RNA kit (MACHEREY-NAGEL, Switzerland) according to the manufacturer's instructions with the following adaptions: Cells were lysed with 350 µl Buffer RA1 and 3.5 µl β-mercaptoethanol (MACHEREY-NAGEL, Switzerland) directly in each well of a 6 well dish. The RNA was eluted in 30-50 µl RNase-free H_2O only.

6.3.2 Reverse transcription polymerase chain reaction (reverse transcription PCR)

The High-Capacity cDNA Reversse Transcription Kit (Applied Biosystem) was used for reverse transcription. First, the RNA concentration of the samples was determined by a spectrophotometer. The reverse transcription master mix, containing 2 µl of 10x RT buffer, 1 µl RT random primers, 0.4 µl dNTPs (100 mM) and 0.5 µl MultiScribe® reverse transcriptase for each reaction, was prepared on ice. Then, 3.9 µl of the master mix was added to 200 ng of RNA diluted in 16.1 µl ddH_2O and kept on ice. The samples were placed into a thermal cycler and the following program was run: 10 min at 26°C, 2 h at 37°C and 5 min at 85°C. Afterwards, the samples containing cDNA were cooled down to 4°C and kept on ice.

6.3.3 qRT-PCR

To analyze gene expression, qRT-PCR was performed using the KAPA SYBR® FAST Universal qPCR Kit (KAPA BIOSYSTEMS). First, the master mix, containing 5 µl Syber Green, 0.8 µl of the primers (Table 5) (1.5 µM forward primer, 1.5 µM reverse primer) and 2.2 µl ddH_2O for each reaction, was prepared for all samples and transferred to quantitative qRT-PCR tubes (Labgene). Then, the cDNA of the reverse transcription was diluted 15-fold in ddH_2O and 2 µl of the diluted cDNA was added to 8 µl of master mix. Four standards (1:10, 1:100, 1:1'000 1:10'000), water as a no template control and a no reverse transcription control were pipetted for each quantitative RT-PCR. The samples were placed into a qRT-PCR cycler (QIAGEN), and 40 cycles were run with the following thermal conditions: denaturation for 3 s at 95°C and extension for 20 s at 60°C using the green channel (excitation: 470 nm, detection 510 nm) for detection. After the 40 cycles, the temperature was

increased to 100°C, which is above the melting temperature of the primers and at which dsDNA denatures and becomes single-stranded, where the dye dissociates. The reaction efficiency, sensitivity and the melting curve were analyzed for each sample at the end of the qRT-PCR run.

6.3.4 Overlapping PCRs

4 different primers were designed for each mutation in mARH1 and hARH1 (Table 5). To amplify the whole fragment, an outer forward primer and an outer reverse primer were designed together with a reverse as well as a forward cluster primer encoding the mutation on the 5'-end (alanine mutated to aspartic acid) and at least 16 nucleotides at the 3'-end, which allowed proper binding to the template. 2 products were separately amplified using one flanking primer (e.g., outer forward/outer reverse) and one mutation primer (e.g., cluster reverse/cluster forward) for the first PCR. For each mutation, 2 PCRs were pipetted in a 50 μl reaction with the reagents of the Phusion® High-Fidelity DNA Polymerase kit (New England Biolabs) (10 μl 5X Phusion HF or GC Buffer, 1 μl dNTPs (10 mM), 2.5 μl forward primer (10 μM), 2.5 μl reverse primer (10 μM), 3.5 ng template (human ARH1, murine ARH1), 1.5 μl DMSO and 0.5 μl Phusion DNA Polymerase in ddH2O). The PCR was run with the following program: initial denaturation for 30 s at 98°C, followed by 35 cycles with 10 s at 98°C, 15 s at 60°C and 15 s at 72°C, and a final extension at 72°C for 10 min. Then, the products were loaded onto a 1% agarose gel (Promega) and separated by 90 V in 1X TAE (40 mM Tris acetate, 1 mM EDTA, and 0.1% acetic acid), cut out and isolated. The different products were then used as template in a second overlapping PCR reaction with the flanking primers. The following reagents from New England Biolabs (10 μl 5X Phusion HF or GC Buffer, 1 μl dNTPs (10 mM), 2.5 μl forward primer (10 μM), 2.5 μl reverse primer (10 μM), 3.5 ng template (human ARH1, murine ARH1), 1.5 μl DMSO and 0.5 μl Phusion DNA Polymerase in ddH2O) were used for the overlapping PCR. The overlapping PCR program included the following steps: initial denaturation for 30 s at 98°C, followed by 35 cycles of 10 s at 98°C, 30 s at 60°C and 30 s at 72°C, and final extension at 72°C for 10 min. 5 μl of the products were loaded on an 1% agarose to check the amplicons.

6.3.5 Agarose gel

An agarose gel was used to separate DNA molecules according to their size. First, the agarose gel apparatus was cleaned with 70% ethanol and then assembled. A 1% agarose gel (Promega) was prepared followed by loading of a lambda marker and samples onto the gel. The DNA was separated for 1 h at 90-100 V in 1x TAE. The bands were visualized using UV light.

6.3.6 Agarose gel extraction of DNA

NucleoSpin® Gel and PCR Clean-up Columns (MACHEREY-NAGEL GmbH & Co, Switzerland) were used for extracting DNA from the agarose gel according to the manufacturer's instructions with the following adaptions: The elution was done in a fresh 1.5 ml Eppendorf tube by adding 3 times 20 μl of 70°C preheated NE buffer (MACHEREY-NAGEL GmbH & Co, Switzerland) to the column and incubating for 5 min at 70°C before centrifugation at RT for 1 min at 11'000 x g.

6.3.7 Restriction endonuclease digest

Restriction endonuclease digestion was performed to prepare sticky ends of the amplified DNA fragments for cloning. The inserts and the plasmid vectors were digested with 2 suitable restriction enzymes (New England Biolabs: BamHI, XhOI, EcoRI) to get the product ends of interest. All enzymes were used with the recommended buffers according to the protocols of New England Biolabs.

6.3.8 Ligation of DNA fragments into a vector

DNA fragments were purified with NucleoSpin® Gel and PCR Clean-up columns after the restriction endonuclease digest. For the ligation reaction, approximately 30 ng of the digested vector and 90 ng of the digested insert, 1 μl Thermo Scientific T4 Ligase (Thermo Scientific), 2 μl of 10x T4 DNA Ligase Buffer (Thermo Scientific), 0.5 μl ATP (10 mM) and ddH_2O were mixed together to a final volume of 20 μl and incubated for 1 h at 22.5°C. The ligation was immediately used for transformation.

6.3.9 Plasmid isolation by miniprep

One bacterial colony was picked and inoculated in 2 ml LB with the corresponding antibiotic overnight at 37°C and 230 rpm in the shaker for each miniprep. The next morning, the culture was centrifuged for 1 min at 16'200 rcf and 4°C. The bacteria pellet was resuspended in 250 μl RES-buffer (MACHEREY-NAGEL, Switzerland). 250 μl of LYS-buffer (MACHEREY-NAGEL, Switzerland) was added to lyse the bacteria. The samples were inverted 5-10 times and then incubated for 5 min on the bench at RT. Directly after these 5 min, 350 μl NEU-buffer (MACHEREY-NAGEL, Switzerland) was added to stop the lysis. The samples were inverted twice, incubated on ice for 10 min and centrifuged for 15 min at 16'200 rcf and 4°C. 800 μl of the supernatant containing DNA was transferred to 700 μl ice cold isopropanol (Sigma-Aldrich), inverted and incubated on ice for 10 min. The precipitated DNA was spun down for 15 min at 16'200 rcf and 4°C. The DNA pellet was washed with ice-cold ethanol (70%) and then dried at RT. The DNA was resuspended by adding 60 μl ddH_2O. The concentration of the DNA was measured by a spectrophotometer.

6.3.10 Plasmid isolation by midiprep

The transformation with plasmids was done after a test-digest and checking the sequence of the plasmid DNA. 1 μl plasmid was added to 50 μl XL-10 *E. coli* and grown overnight in 120 ml LB with the corresponding antibiotic for an appropriate selection at 37°C and 230 rpm. The plasmid DNA was purified from the culture using NucleoBond® Xtra Midi (MACHEREY-NAGEL, Switzerland) according to the manufacturer's instructions.

6.4 Protein-based methods

6.4.1 Nuclear and cytosolic extract

Cells were seeded and transfected with plasmid DNA after 1 day. Cells were harvested into a 15 ml falcon tube 48 h after transfection at a confluency of 70-100%. Then, cells were centrifuged at 210 rcf and 4°C for 5 min. The supernatant was discarded and the pellet washed with 10 ml ice-cold 1 x PBS and centrifuged again. The cell pellet was first transferred to a 1.5 ml Eppendorf with a cut pipet tip. The pellet was then washed twice by resuspending it with 1 ml of Buffer A (1 M HEPES, 1 M $MgCl_2$, 3 M KCl, 0.2 M PMSF, 1 mg/ml pepstatin, 1 mg/ml leupeptin, 1 mg/ml bestatin) followed by centrifugation at 400 rcf

and 4°C for 1 min. The supernatant was removed and the pellet was resuspended in 3 volumes of Buffer A+ (Buffer A + 10% NP-40) and incubated for 7-10 min until the cell membrane was broken. After the incubation, the lysed cell suspension was centrifuged for 5 min at 9'600 rcf and 4°C, which resulted in cytosolic extract as supernatant and the pellet containing the nuclei. The pellet was leaved intact during the washing with 1 ml Buffer A, which was followed by a centrifugation at 100 rcf for 1 min at 4°C. To lyse the nuclear membrane, the pellet was resuspended in 3 volumes Buffer C (1 M HEPES, 5 M NaCl, 1 M $MgCl_2$, 30% glycerol (87%), 0.2 M PMSF, 1 mg/ml pepstatin, 1 mg/ml leupeptin, 1 mg/ml bestatin) and incubated on a roller shaker at 4°C for 15-20 min. Then, the suspension was centrifuged for 5 min at 18'800 rcf and 4°C, which yielded the nuclear extract in the supernatant. The salt concentrations of the extracts were adjusted to a salt concentration of 150 mM with either 5 M NaCl for cytosolic extracts or Buffer D (1 M HEPES, 0.2 M PMSF, 1 mg/ml pepstatin, 1 mg/ml leupeptin, 1 mg/ml bestatin) for nuclear extracts. Glycerol was added to the extracts to a final concentration of 20%. The protein concentration was determined by Bradford protein assay. The extracts were shock-frozen in liquid nitrogen and stored at -80°C.

6.4.2 Whole cell extract

Cells were seeded and transfected the following day with plasmid DNA. Cells were harvested into a 15 ml falcon tube 48 h after transfection at a confluence of 70-100% and centrifuged at 210 rcf and 4°C for 5 min. The supernatant was discarded and the pellet washed with 10 ml ice-cold 1 x PBS and centrifuged again. The supernatant was discarded and the pellet resuspended in 5 volumes of lysis buffer (50 mM Tris-HCl pH 8.0, 125 mM NaCl, 0.5% NP-40, 0.5 mM DTT, 0.5 mM PMSF, 1 μg/ml leupeptin, 1 μg/ml pepstatin, 1 μg/ml bestatin). The suspension was incubated on a roller shaker at 4°C for 20-30 min and then again centrifuged at 4°C at 18'800 rcf for 10 min, which yielded the whole cell extract in the supernatant. Glycerol was added to the whole cell extract to a final concentration of 10%. The concentration of the whole cell extract was determined by Lowry protein assay. The extracts were shock-frozen in liquid nitrogen and stored at -80°C.

6.4.3 Purification of recombinant proteins

For purification of recombinant proteins, was done a transformation of BL 21 gold *E. coli*. To induce expression of protein, IPTG was added to the transformation, which was again incubated for 3 h. After the incubation, the 400 ml BL 21 gold *E. coli* culture was centrifuged for 30 min at 2'700 g and 4°C. The pellet was resuspended in 20 ml binding buffer (0.05 M Tris-HCl pH 7.4, 0.3 M NaCl, 0.1% NP-40, 5% glycerol, 1 mM DTT, 2 mM PMSF, 1 µg/ml leupeptin, 1 µg/ml pepstatin, 1 µg/ml bestatin) and cells then lysed using a French press. Cell debris was centrifuged at 4'000 rcf and the supernatant containing proteins transferred to a fresh Falcon tube. 250 µl glutathione sepharose 4B beads (GE healthcare) were used per sample and equilibrated in binding buffer for 5 min on a roller in the cold room and then centrifuged for 5 min at 100 rcf. Beads were added to the extract and filled up with binding buffer to a final volume of 40 ml. Binding was done for 1.5 h in the cold room on a roller. After binding, the bound protein was spun down at 120 rcf and 4°C and washed 3 times with 15 ml wash buffer (0.05 M Tris-HCl pH 7.4, 0.4 mM NaCl, 1% NP-40, 5% glycerol, 1 mM DTT, 2 mM PMSF, 1 µg/ml leupeptin, 1 µg/ml pepstatin, 1 µg/ml bestatin) and centrifuged at 120 rcf and 4°C. Beads were transferred to an 1.5 ml Eppendorf tube and washed once for 10 min on a roller in the coldroom with elution buffer without glutathione (0.05 M Tris-HCl pH 8, 0.05 M NaCl, 5% glycerol, 1 mM DTT, 2 mM PMSF, 1 µg/ml leupeptin, 1 µg/ml pepstatin, 1 µg/ml bestatin). After the wash with elution buffer, beads were centrifuged at 1'000 rcf and 4°C for 5 min. Protein was eluted 3 times with 500 µl elution buffer with glutathione (0.05 M Tris-HCl pH 8, 0.05 M NaCl, 5% glycerol, 1 mM DTT, 2 mM PMSF, 1 µg/ml leupeptin, 1 µg/ml pepstatin, 1 µg/ml bestatin, 0.02 M glutathione) by rolling for 20 min on a roller in the cold room and centrifugation at 1'000 g and 4°C for 5 min. The protein concentration was determined by Bradford protein assay.

6.4.4 Immunoprecipitation (IP)

Flag-tagged proteins were immunprecipitated using ANTI-FLAG M2 Magnetic Beads (Sigma-Aldrich). The salt concentration of the protein extracts was first adapted to a salt concentration of 150 mM NaCl with 5 M NaCl. 30 µl slurry (50% beads) per 500 µg protein extract were transferred to a tube and beads equilibrated by resuspending with 5 packed gel volumes of Buffer A+ (1 M HEPES, 1 M $MgCl_2$, 3 M KCl, 0.2 M PMSF, 1 µg/ml leupeptin, 1 µg/ml pepstatin, 1 µg/ml bestatin, 10% NP-40) 3 times for 5 min on a roller in the cold

room. Buffer A+ was discarded using the appropriate magnetic separator and beads divided into fresh tubes. Protein extracts were incubated with beads in a final volume of 2 ml, filled up with Buffer A+. Binding was done for 2 h on a roller in the cold room. After the binding reaction, magnetic beads were collected by placing the tube in the appropriate magnetic separator and removing the supernatant. The supernatant of the binding was kept as flow through. The beads were washed 3 times with 2 ml TBS (50 mM Tris HCl pH 7.4, 150 mM NaCl, 1 μg/ml leupeptin, 1 μg/ml pepstatin, 1 μg/ml bestatin) to remove nonspecifically bound proteins. Each supernatant was kept as wash. Beads were either mixed with SDS-loading buffer and boiled for 5 min at 95% or eluted with 3x Flag peptide (Sigma-Aldrich, Catalog Number F4799) according to the manufacturers protocol.

6.4.5 In vitro ADP-ribosylation assay

β-Actin was radioactively MARylated on arginine *in vitro* as a substrate for the ADP-ribosyl hydrolase assay. 2 µg β-actin was incubated with 100 ng recombinant 50 ng CDTa in the presence of 100 nM ^{32}P NAD^{+}, 150 μM cold NAD^{++}and reaction buffer (5 mM HEPES, pH 7.5, 0.1 mM $CaCl_2$, 0.5 mM NaAc, 0.1 mM ATP) in a total volume of 15 µl per reaction for the ADP-ribosylation. CDTa reactions were incubated for 30 min at 37 °C. The reaction was stopped by filtration through a G50 column (GE Healthcare) according to the manufacturers protocol. De-ADP-ribosylation reactions were performed with either 10 pmol hPARG, hARH1, or mARH1 wt or mut protein in demodification buffer (250 mM Tris, 20 mM $MgCl_2$, 1.25 mM DTT) in a total volume of 25 1 μg/ml leupeptin, 1 μg/ml pepstatin, 1 μg/ml bestatin l at 30 °C for 17 h and stopped by adding SDS-PAGE loading buffer and boiling for 5 min at 95°C. De-ADP-ribosylation of β-actin was visualized by SDS-PAGE and autoradiography.

6.4.6 Bradford protein assay

5x BIO-RAD Protein assay solution (Bio-Rad Laboratories GmbH) was diluted to 1x with ddH_2O. As standards, 20 μl BSA solutions (0.19 mg/ml, 0.376 mg/ml, 0.528 mg/ml and 0.69 mg/ml) in 1 ml of 1x BIO-RAD solution were used. 2-20 μl of protein extract was added to 1 ml 1x BIO-RAD solution to determine their protein concentration. The absorbance was measured at 595 nm with a spectrophotometer and the protein concentration determined based on the BSA standard curve.

6.4.7 Lowry protein assay

The Lowry protein assay was used to determine protein concentrations of extracts containing reagents incompatible for the Bradford assay. The Lowry solution was prepared freshly by mixing 2 different solutions (Solution A: 47 mM Na_2CO_3, 100 mM NaOH in H_2O, Solution B: 0.5% CuSO4, 0.05% sodium citrate in H_2O at a ratio of 50:1) the day of the measurement. First, 10 μl of protein extract was diluted in 90 μl ddH_2O or 50 μl BSA standard solution (0.19 mg/ml, 0.376 mg/ml, 0.528 mg/ml and 0.69 mg/ml) was diluted with 50 μl ddH_2O. 100 μl of the diluted samples were added to 1 ml of the Lowry solution and incubated for 10 min at room temperature. 100 μl of 1:3 diluted Folin & Ciocalteus phenol was added to the protein mixture, vortexed and again incubated for 30 min at RT in the dark. The absorbance was measured at 595 nm with a spectrophotometer and the protein concentration calculated based on the BSA standard curve.

6.4.8 Sodium Dodecyl Sulfate (SDS) Polyacryl Amide Gel Electrophoresis (PAGE)

SDS-PAGE was used to separate proteins according to their electrophoretic mobility, which is determined by the size, the conformation and charge of the molecule. First, the SDS-PAGE apparatus was cleaned with 70 % ethanol and assembled. A glass and a teflon plate (10 x 8.5 cm) separated by 2 spacers (10 x 0.15 cm) were fixed into a gel preparation unit. First, the separation gel solution (7.5% SDS-PAGE: 4.5 ml ddH_2O, 2 ml Solution B (1.5 M Tris-HCl pH 8.8, 0.4% Na-dodecyl sulfate), 2 ml 40% acrylamide solution (37.5:1 Acrylamide-Bis, SERVA Electrophoresis GmbH), 80 μl 10% APS, 8 μl TEMED; 10% SDS-PAGE: 4 ml ddH_2O, 2 ml Solution B, 1.5 ml 40% acrylamide solution, 80 μl 10% APS, 8 μl TEMED; 12% SDS-PAGE: 3.6 ml ddH_2O, 2 ml Solution B (1.5 M Tris-HCl pH 8.8, 0.4% Na-dodecyl sulfate), 2.4 ml 40% acrylamide solution, 80 μl 10% APS, 8 μl TEMED was filled in between the 2 plates. Some ddH_2O was added to the top of the separation gel to guarantee a sharp border. After, polymerization of the separation gel, the layer of H_2O was removed and replaced by the stacking gel (4.5%: 3.15 ml ddH_2O, 1.25 ml Solution C (0.5 M Tris-HCl pH 6.8, 0.4% (w/v) Na-dodecyl sulfate and a tip of bromophenol blue), 0.6 ml 40% acrylamide solution, 0.05 ml 10% APS, 0.005 ml TEMED). A comb with 10 or 15 flaps was placed into the stacking gel. After polymerization, the gel was placed into the running apparatus, which was filled with 1x SDS running buffer (25 mM Tris base, 200 mM glycine, 0.1% (w/v) Na-dodecyl sulfate). 3 μl of PageRuler^{TM} as marker for the molecular weight was added into one

pocket of each gel. The remaining pockets were filled with different protein samples previously boiled for 5 min at 95°C. The gel was run for 30 min at 90 V and afterwards at 130 V until the sample buffer reached the end of the separation gel. The gel was disassembled and either stained with Coomassie, blotted or used for silver staining.

6.4.9 Western blot analysis

After the separation of proteins by SDS-PAGE, the proteins were transferred to a nitrocellulose membrane to detect proteins by Western blot. A Western blot unit, existing of 2 wetted sponges and 2 prewetted Watman papers surrounding each side of the PVDF membrane (0.45 µm, activated in 100% ethanol) and the SDS-gel, was assembled in a plastic frame and put into a Western blot chamber filled with 1x transfer buffer (20% methanol, 70% ddH_2O, 10% 10x transfer buffer, 25 mM Tris-base, 192 mM glycine, dissolved in ddH_2O) and an ice block. Blotting was performed at 130 V and 4°C for 1 h or overnight at 30 V and 4°C, followed by 1 h at 100 V. The membrane was stained with Ponceau red (1% Ponceau S in 0.1% acetic acid) and destained with ddH_2O to check blotting. The membrane was blocked in blocking solution (5% skim milk in TBST: 10 mM Tris-HCl pH 7.5, 150 mmol NaCl, ddH_2O, 0.1% Tween-20) on a shaker at RT for 1 h. After blocking, the membrane was incubated on a roller shaker for 1 h with the primary antibody (Table 3) in 1% skim milk (for antibodies, see materials). The membrane was washed 3 times before adding the secondary antibody (Table 3) 1:15'000 in TBS-T (for antibodies, see materials), with TBST for 5 min. The blot was washed again 3 times with TBS-T for 5 min and analyzed on an Odyssey® Imager.

6.5 Microbiological Methods

6.5.1 Transformation of chemocompetent *E. coli*

For transformation, 1 µg plasmid DNA was added to 50 1 µg/ml leupeptin, 1 µg/ml pepstatin, 1 µg/ml bestatin 1 freshly thawed chemocompetent *E. coli* (strain XL-10 for plasmid amplification or BL21 gold for protein expression) and incubated on ice for 30 min to 1 h. The bacteria were then heat-shocked for 45 s at 42°C on a heat block. After the heat shock, the bacteria were put on ice for 2 min and incubated for 1 h at 37°C and 90 rpm in 250 µl LB media. The transformation was either plated onto an LB Agar-plate containing the appropriate antibiotic (50 µg/ml ampicillin or kanamycin, depending on the plasmid) or

added to 50 ml LB medium containing the appropriate medium. The next day, bacterial colonies were picked and inoculated into 2 ml LB-medium with 50 μg/ml antibiotics overnight at 37°C or the bacteria of the LB-medium was used for MiniPrep, MidiPrep or for protein purification.

For protein purification, the culture was put into 400 ml LB-medium containing the appropriate antibiotic (50 μg/ml) and incubated until the OD at 600 nm reached a value between 0.4 and 0.6. 400 μl of 1 M IPTG was added to the culture to activate protein expression and the transformation reaction again incubated at 30°C and 230 rpm for 3 h.

7 Results

7.1 ARH1 and ARH3, but not ARH2, are expressed in NIH3T3 fibroblasts

In order to detect whether NIH3T3 fibroblasts, which are responsive to LPS pro-inflammatory signaling, express the ADP-ribosylhydrolases ARH1, ARH2, or ARH3, the mRNA levels of all three ARH family members were analyzed in NIH3T3 cells. The total RNA was isolated from untreated, siMock treated and cells treated with siRNA against ARH1, ARH2 and ARH3 to knockdown their potential mRNA. The RNA was subsequently reverse transcribed and quantified by qRT-PCR. While the RNA levels of ARH1 and ARH3 were nicely detectable by qRT-PCR and efficiently knocked down after 2 days using the respective siRNAs (Figure 9B), ARH2 was not detectable. To confirm that the selected primers for detection of ARH2 are functional, the same primers were tested using cDNA generated from RNA of heart myocytes of mice, since ARH2 is expressed in this tissue (biogps.org).

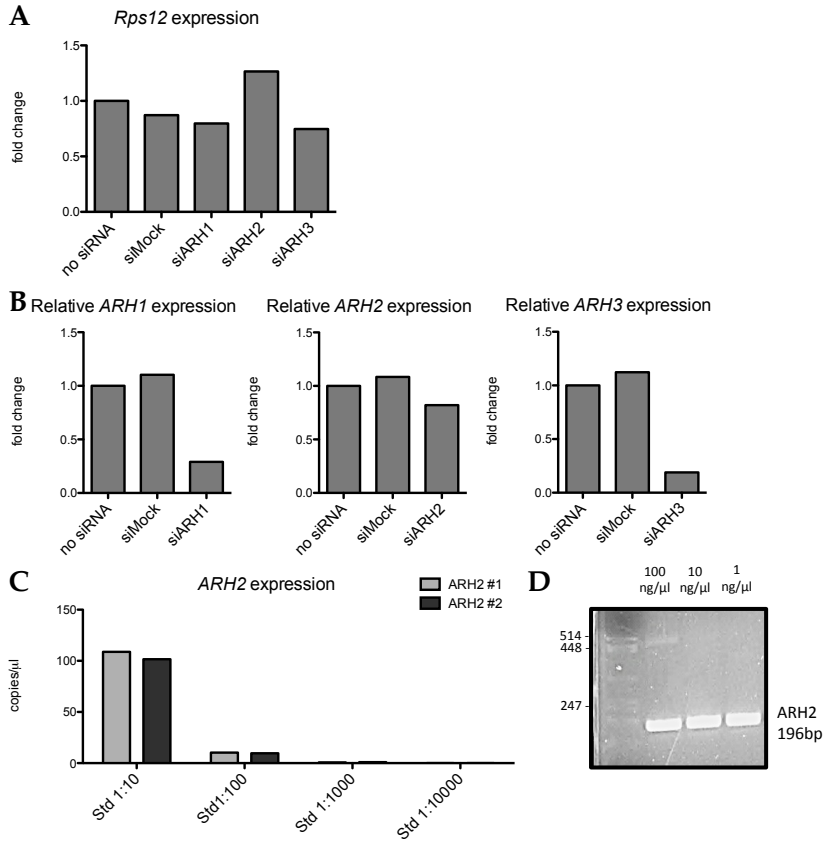

Figure 9: *ARH1* and *ARH3*, but not *ARH2*, are expressed in NIH3T3 cells. A: Expression levels of *Rps12* B: Expression levels of *ARH1*, *ARH2* and *ARH3* in NIH3T3 cells treated with siMock, siARH1, siARH2 and siARH3. C: Expression of *ARH2* in mouse heart myocytes measured with two different primer pairs (ARH2#1 ARH2#2). D: Agarose gel of amplicon generated by qRT-PCR with primers for ARH2 on mouse heart myocytes. This experiment was performed once.

A plasmid containing cDNA from ARH2 was used to generate the standard curve. As expected, ARH2 was nicely detected in heart myocytes (Figure 9C-D), confirming that the primer pair for ARH2 is functional and suggesting that ARH2 is not expressed in NIH3T3 cells. Taken together, NIH3T3 cells seem to be a suitable cell line for investigating a potential role of ARH1 and ARH3 during pro-inflammatory stimulation. Due to the fact that we were mainly interested in MARylation, only ARH1 was further investigated.

7.2 ARH1 dampens the expression of *iNOS* after LPS stimulation

To investigate whether and in which direction ARH1 influences NF-κB dependent gene expression, *ARH1* was knocked down in NIH3T3 cells by siRNA and cells were subsequently stimulated with LPS or LPS together with IFNγ for 4 h before RNA was isolated and reverse transcribed. NIH3T3 cells transfected with siMock served as knockdown control. The knockdown of ARH1, as well as the expression levels of *IL-6*, *IP-10* and *iNOS,* were quantified by qRT-PCR and normalized against *Rps12,* whose expression did not change under the tested condition. LPS induced all analyzed NF-κB target genes, although to a different level (Fig. 10B-D). The addition of IFNγ slightly enhanced the LPS-induced gene expression (Figure 10B-D). Knockdown of ARH1 did not affect the expression of *IL-6* (Figure 10B), but enhanced the expression of *IP-10* (Figure 10C) slightly and the expression of *iNOS* (Figure 10D) tremendously.

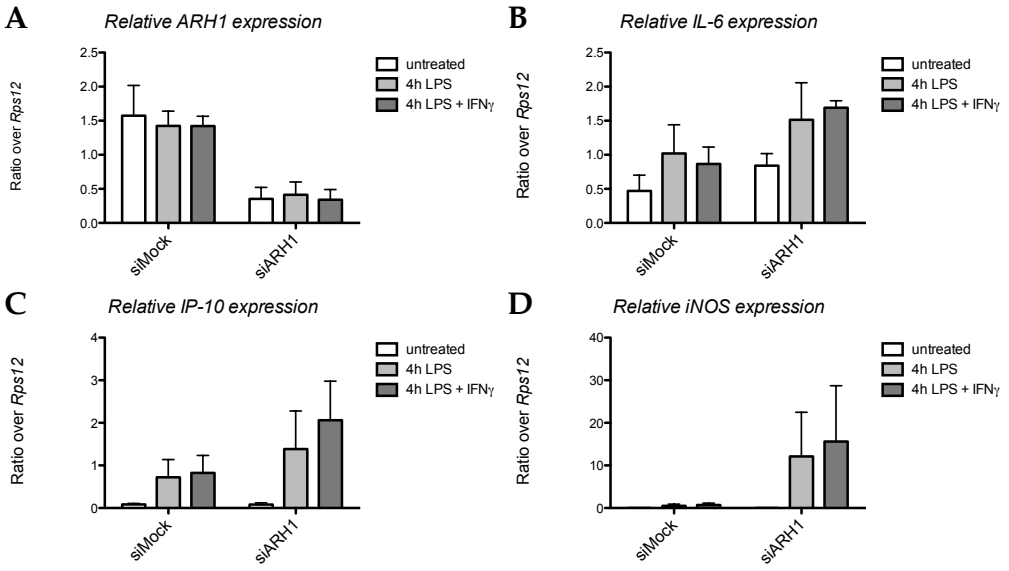

Figure 10: Knockdown of ARH1 in NIH3T3 cells enhances the expression of LPS or LPS + IFNγ induced *iNOS* and *IP-10*. NIH3T3 cells were transfected with siMock and siARH1 and treated with LPS or LPS + IFNγ for 4 h. A: *Rps12* expression levels (mean of three independent experiments). B: Relative *ARH1* expression levels, C: Relative *IL-6* expression levels, D: Relative *IP-10* expression levels and E: Relative *iNOS* expression levels. Mean of three independent experiments.

These data indicated that ARH1 only affects the expression of certain NF-κB target genes after LPS stimulation, and that the regulation is rather a dampening effect.

7.3 Cloning of mARH1 and hARH1 wildtype (wt) and an enzymatic mutant (mut) in different expression vectors

To investigate whether the enzymatic activity of ARH1 is involved in the observed dampening of *iNOS* expression, human and mouse ARH1 (hARH1 and mARH1) wt and the enzymatically inactive mut of ARH1 were all cloned into mammalian expression vectors pcDNA3.1 and pHA-MEX. The open reading frames were generated by PCR (for wt) or overlap PCR (for the mut) from a plasmid containing mARH1 (kindly provided by J. Moss) or hARH1 (bought from Biocat) introducing two amino acid changes (mouse: D61/62A, human D55/56A) according to previous reports [4]. The generated PCR fragments were subsequently cloned into the mammalian expression vectors pcDNA3.1 (for a N-terminal Flag-tagged version) and pHA-MEX (for a N-terminal HA-tagged version) using the restriction enzymes BamHI and XhoI (Figure 11A-B).

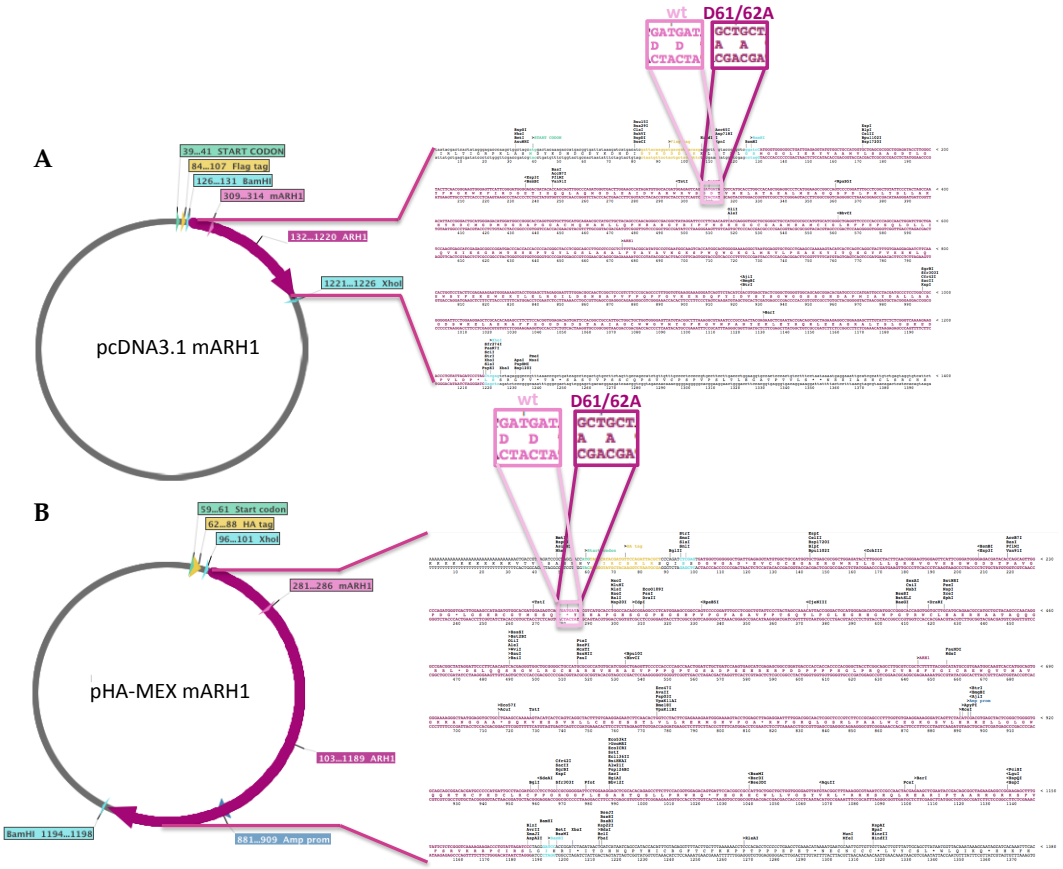

Figure 11: Vector maps of the pcDNA3.1 and pHA-MEX eukaryotic expression plasmids for mARH1. mARH1 and hARH1 constructs were all cloned as described in the text. A) pcDNA3.1 with a Flag-tag at the N-terminal end (yellow: N-terminal Flag-tag, turquoise: BamHI and XhoI restriction sites, pink: mARH1) or B: pHA-MEX with a HA-tag at the N-terminal end (yellow: N-terminal Flag-tag, turquoise: BamHI and XhoI restriction sites, pink: mARH1) hARH1 wt and mut constructs are the same like mARH1.

To confirm that the generated ARH1 mut (mouse: D61/62A or human D55/56A respectively) is indeed enzymatically inactive, due to the inability to bind Mg^{2+}[4], mARH1 and hARH1 wt and mut were also cloned into the pGEX-2T vector. Since the hARH1 wt and mut and mARH1 wt plasmids were already cloned by Jeannette Abplanalp (DMMD, UZH), only the mARH1 mut had to be additionally cloned into a bacterial expression vector. The open reading frame of mARH1 mut was cloned into the GST-tagged vector using the restriction enzymes BamHI and EcoRI (Figure 12A). The cloning and the presence of the ARH1 mutation were confirmed by sequencing the plasmid. GST-tagged expression plasmids of mARH1 wt and mut as well as their human counterpart were transformed into BL21 gold *E. coli*, expressed upon IPTG induction and purified by batch purification using glutathione sepharose beads. The newly cloned GST-tagged mARH1 mut (as representative of the four constructs) was nicely expressed and eluted by glutathione from the beads (Figure 12B).

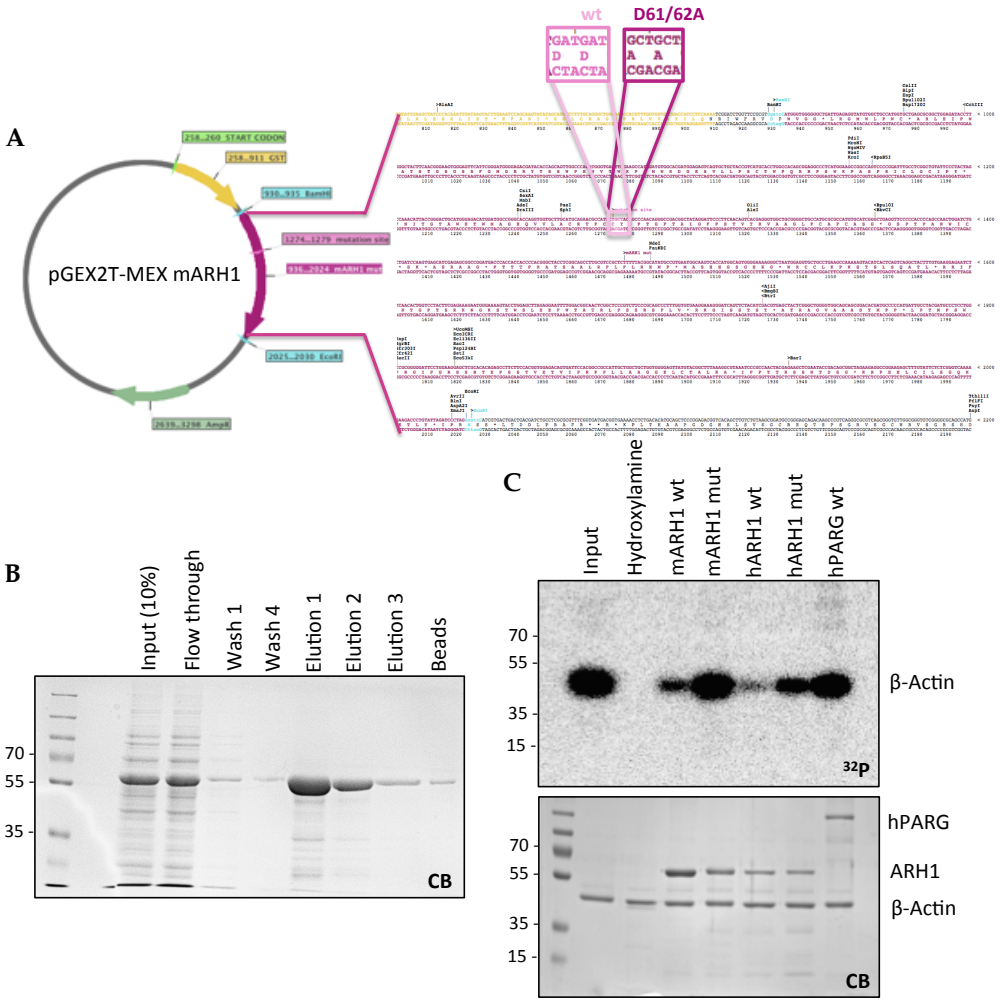

Figure 12: GST-tagged mARH1 mut (D61/62A) and hARH1 mut (D55/56A) are enzymatic inactive. A: Map of the cloned GST-tagged mARH1 D61/62A mut (grey: pGEX-2T vector, yellow=GST-tag, turquoise: BamHI and EcoRI restriction sites), violet: ARH1 mutant sequence). B: Coomassie blue-stained SDS-gel of fraction from the expression and purification of GST-tagged mARH1 mut from BL 21 gold *E. coli*. C: X-ray exposure of the coomassie-stained SDS-gel of the enzymatic *in vitro* assay of ARH1 using arginine MARylated β-actin. hPARG served as negative control, Hydroxylamine as positive control. This is a representative example of 2 independent experiments.

To test the enzymatic activity of hARH1 and mARH1 wt and mut, β-actin was first ADP-ribosylated by *Clostridium difficile* transferase ToxA (CDTa, published to trans-ADP-ribosylate actin at A177 [59]) and subsequently separated from the toxin and NAD^+ using a G50 column. While hARH1 and mARH1 wt proteins nicely removed the modification of β-actin, the respective mutants (hARH1 D55/56A and mARH1 D61/62A) were not able to do so. To confirm that the observed reaction was specific towards the modified non-ADP-riboslyated arginine, hPARG, which only removes PAR, was used as a negative control and hydroxylamine, which chemically hydrolyzes arginine ADPr linkages, as a positive control (Figure 12C). Together, these data indicate that the human amino acid residues of D55/56 and murine D61/62 are indeed important residues for the enzymatic activity of ARH1.

7.4 ARH1 wildtype and ARH1 enzymatic mutant localize to the cytoplasm

To functionally test whether the newly cloned ARH1 constructs would express the corresponding full-length proteins, the different vectors for Flag- and HA-tagged mARH1 wt and mut, and pcDNA3.1 and pHA-MEX empty vector (EV) as control, were transfected with calcium phosphate into NIH3T3 cells. Cells were harvested 48 h after transfection, fractionated into nuclear and cytoplasmic extract and proteins subsequently separated by SDS-PAGE (Figure 13). The expression of ARH1 was confirmed by immunoblot analysis using anti-Flag antibody. The immunoblot did nicely detect Flag-tagged mARH1 wt and mut in the cytoplasmic fraction. No Flag-tagged mARH1 wt and mut could be detected in the nucleus, suggesting that ARH1 is localized only in the cytoplasm. The quality of the fractionation was controlled by probing the membrane with an anti-ARTD1 antibody (nuclear protein) or anti-tubulin (cytoplasmic protein).

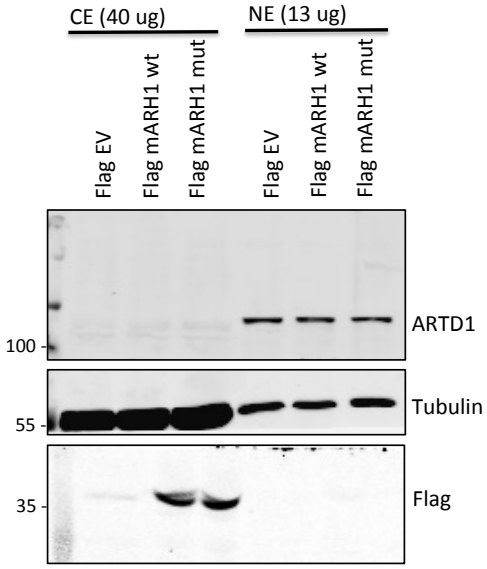

Figure 13: Flag-tagged mARH1 wt and mut are expressed in NIH3T3 cells and localize to the cytoplasm. Immunoblot of nuclear (NE) and cytosolic (CE) extract of NIH3T3 cells transfected with pcDNA3.1 empty vector, Flag-tagged mARH1 wt or mut stained with anti-Flag and anti-ARTD1 as nuclear control and anti-tubulin as cytoplasmic control. This is a representative example of several independent nuclear and cytosolic extracts.

To validate the expression and the localization of Flag- and HA-tagged mARH1 wt and mut in NIH3T3 cells with another readout, immunofluorescence was performed. The expression vectors Flag-tagged mARH1 wt and mut and the HA-tagged mARH1 wt and mut were transfected into NIH3T3 cells by calcium phosphate. pcDNA3.1 empty vector or pHA-MEX empty vectors were used as a control for the Flag and HA staining. After 48 h of transfection,

cells were fixed with paraformaldehyde (PFA) and the localization of mARH1 wt and mut with different tags was assessed by immunofluorescence using the appropriate antibodies. Flag-tagged mARH1 wt and mut were both expressed in NIH3T3 cells and localized to the cytoplasm (Figure 14A). Also HA-tagged mARH1 wt and mut localized to the cytoplasm (Figure 14B), suggesting that mARH1 wt and mut are expressed and localize to the cytoplasm independent of their tag or sequence (wt compared to mutant).

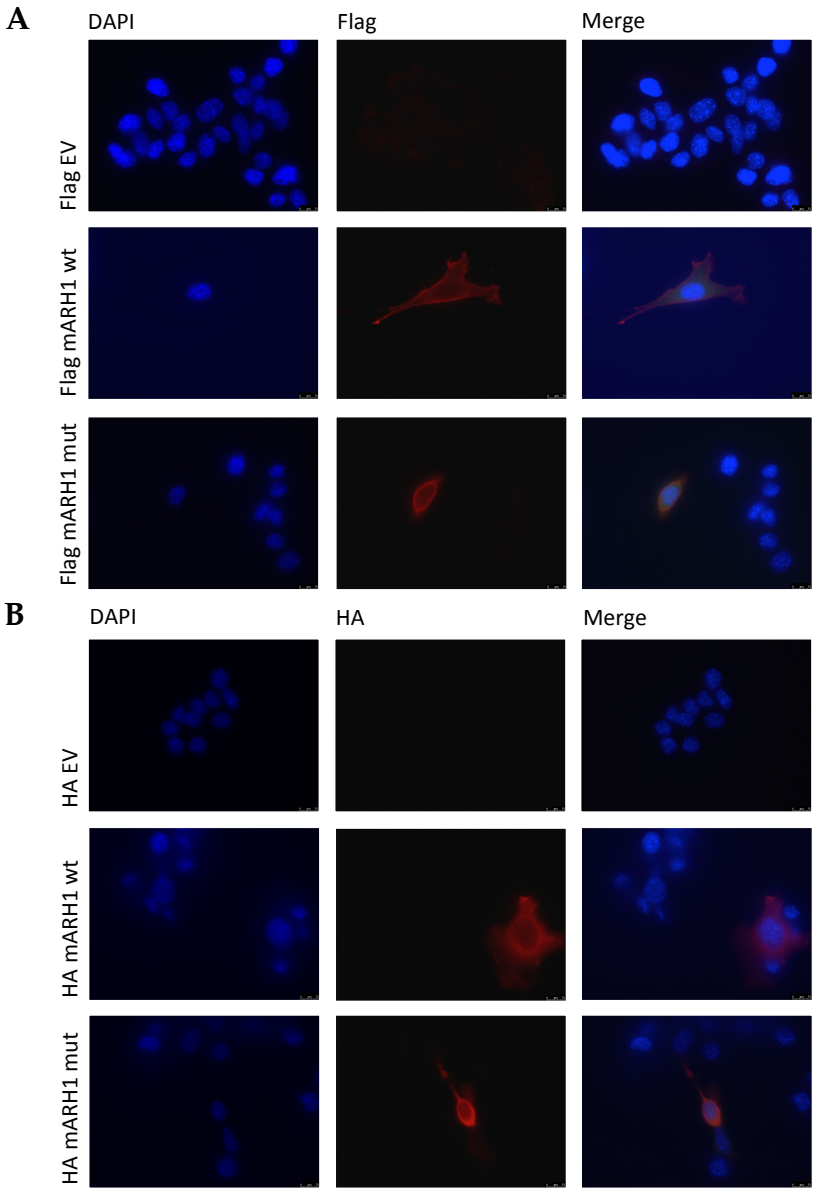

Figure 14: Flag- and HA-tagged mARH1 wt and mut localize to the cytoplasm in NIH3T3 cells. Staining was done with the appropriate antibodies (anti-Flag/anti-HA) and DAPI by mounting with VECTASHIELD antifade mounting medium. Flag and pHA-MEX empty vector (EV) serve as antibody control. A: Flag-tagged mARH1 wt and mut. B: HA-tagged mARH1 wt and mut. This is a representative example of two independent immunofluorescences.

To confirm that the hARH1 constructs are also expressed in mammalian cells and localize to the same cellular compartment as mARH1, the experiment was repeated using Flag- and HA-tagged hARH1 wt and mut transfected in HEK293 cells. pcDNA3.1 empty vector and pHA-MEX empty vectors were used as a control for the Flag and HA staining. Overall the transfection efficiency was higher in HEK293 cells, compared to NIH3T3 cells (10% versus 50%). The immunofluorescence analysis revealed that also the hARH1 constructs (wt and mut) localize to the cytoplasm (Figure 15A-B), confirming the cytoplasmic localization of ARH1 under basal (untreated) conditions in human cells.

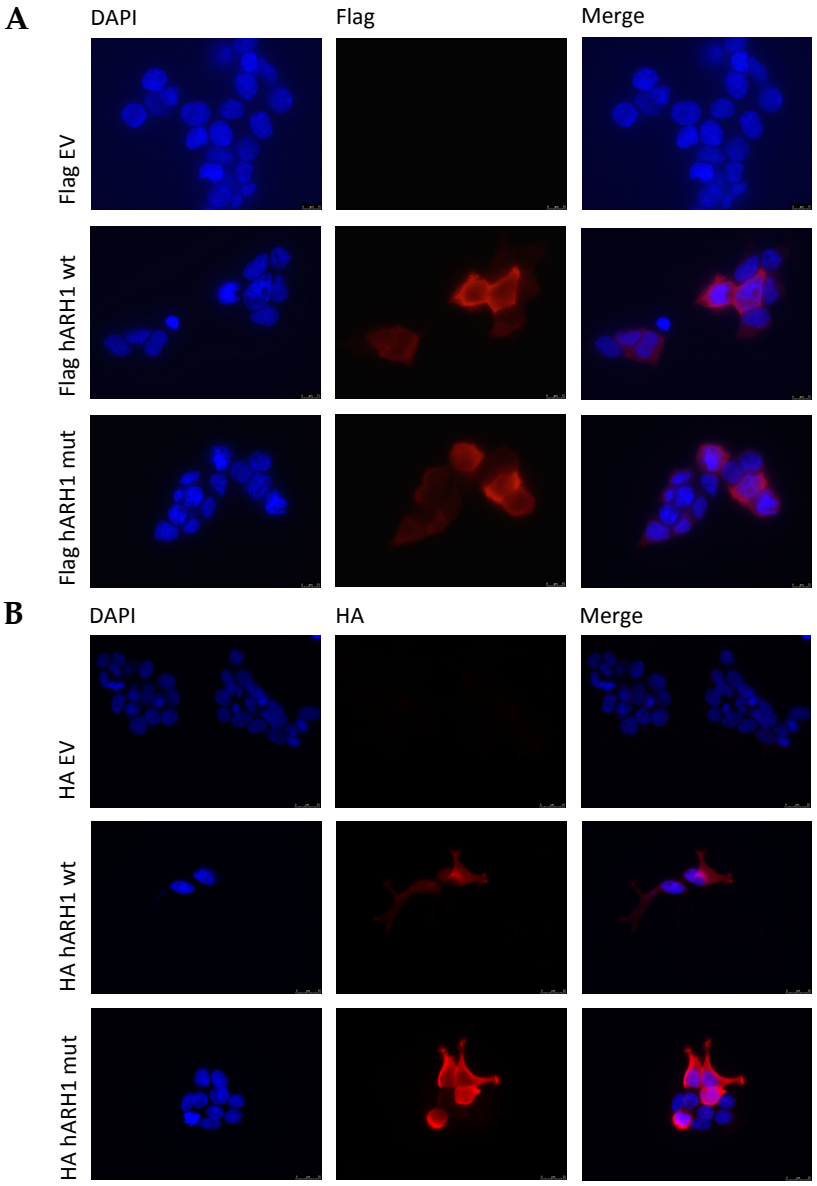

Figure 15: Flag- and HA-tagged hARH1 wt and mut localize to the cytoplasm of HEK293 cells. Staining was done with the appropriate antibodies (anti-Flag/anti-HA) and DAPI by mounting with VECTASHIELD antifade mounting medium. Flag and pHA-MEX empty vector serve as antibody control. A: Flag-tagged hARH1 wt and mut. B: HA-tagged hARH1 wt and mut. This is a representative example of two independent immunofluorescences.

7.5 The enzymatic activity of ARH1 regulates LPS induced *iNOS* expression

To investigate whether the enzymatic activity of ARH1 is involved in the observed dampening of *iNOS* expression after LPS treatment, Flag-tagged mARH1 wt or mut expression vector as well as the pcDNA3.1 empty vector were transfected by calcium phosphate into NIH3T3 cells. 2 days after transfection, NIH3T3 cells were treated with LPS for 4 h to induce expression of NF-κB target genes. RNA was isolated and reverse transcribed to cDNA. The knockdown of ARH1, as well as the expression levels of *IL-6*, *IP-10* and *iNOS* were quantified by qRT-PCR and normalized against *Rps12,* whose expression did not change under the tested conditions. *mARH1* was 3-4-fold overexpressed in cells transfected with Flag-tagged mARH1 wt and mut in comparison to cells transfected with pcDNA3.1 empty vector only, corresponding to the basal *ARH1* levels (Figure 16A). Flag-tagged mARH1 wt repressed the LPS-induced *IL-6* and *IP-10* levels, while Flag-tagged mARH1 mut did not (Figure 16B-C). Although *iNOS* was induced only little, overexpression of ARH1 wt did not allow the induction of *iNOS* also for this sample, while overexpressing the ARH1 mut allowed induced *iNOS* expression (Figure 16D), suggesting that overexpression of ARH1 wt but not ARH1 mut affected the gene expression of *IL-6* and *iNOS*, complementary to what was observed when knocking down ARH1. Moreover, since the ARH1 mut was not able to do so, the enzymatic activity of ARH1 seems to be important for the observed repressory effect of ARH1 on NF-κB dependent signaling.

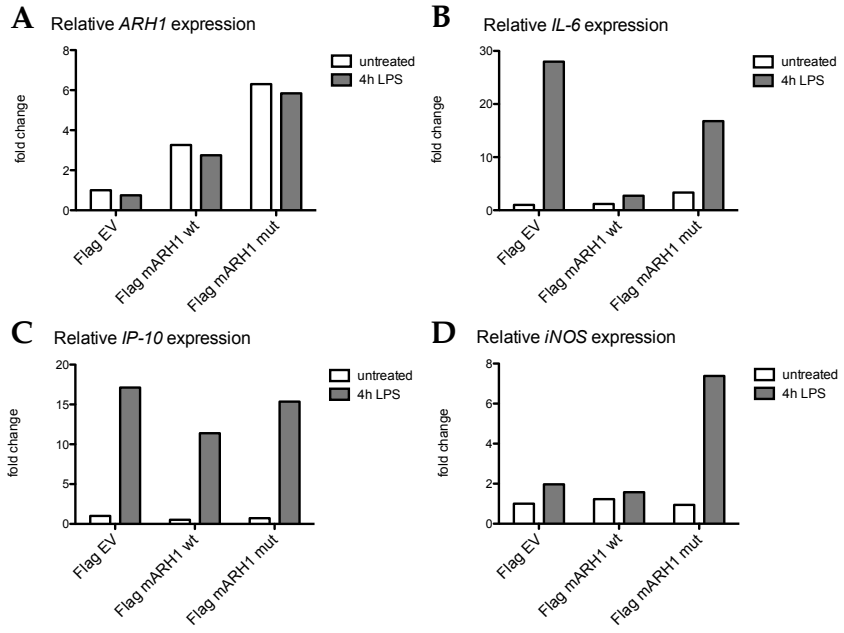

Figure 16: Overexpression of AHR1 wt but not ARH1 mut are repressing the LPS induced expression of *IL-6* or *iNOS*. A: The relative expression levels after transfection of pcDNA3.1 empty vector, Flag-tagged mARH1 wt or Flag-tagged mARH1 mut untreated or stimulated with 4h LPS was measured for *ARH1* (A), *IP-10* (B), *IL-6* (C) or *iNOS* (D). This is a representative example of 2 independent experiments.

Since the overexpressed ARH1 wt and mut might functionally interfere with the endogenously expressed ARH1, ARH1 was first knocked down using the siRNA against the 3'UTR of ARH1 for 24 h followed by the overexpression of ARH1 wt or mut (which were not targeted by the siRNA) for 24 h. pcDNA3.1 empty vector was used as control. After a total of 44 h, NIH3T3 cells were stimulated for 4 h with LPS. RNA was isolated, reverse transcribed to cDNA and the gene expression of NF-κB target genes *iNOS, IP-10* and *IL-6* quantified by qRT-PCR. Knockdown of *ARH1* did nicely work as well as the overexpression of *ARH1 wt* and *ARH1 mut* (Figure 17A). The overexpression of ARH1 wt and mut was as expected detectable in in presence of siRNA against ARH1. The knockdown of ARH1 complemented with the empty vector again allowed at least a 2-fold enhanced inflammatory gene expression of the analyzed genes when compared to siMock (Figure 17B-D). Overall, overexpression of ARH1 wt and mut did not have a huge effect on *IP-10* and *IL-6* expression (Figure 17C and B). *iNOS* expression levels, however, were again repressed when ARH1 wt was overexpressed (in both siMock and siARH1 conditions), compared to the sample with overexpressed ARH1 mut (Figure 17D), suggesting that the knockdown of endogenous *ARH1* enhances the expression of the analyzed NF-κB target genes in general, while an overexpression of Flag-tagged mARH1 wt but not mut decreases the expression of *iNOS* 4 h

after LPS treatment. The observed effect was not as prominent when compared to the experiments shown in Figure 16, which might be explained by a lower transfection rate of the plasmids after siRNA treatment of the cells.

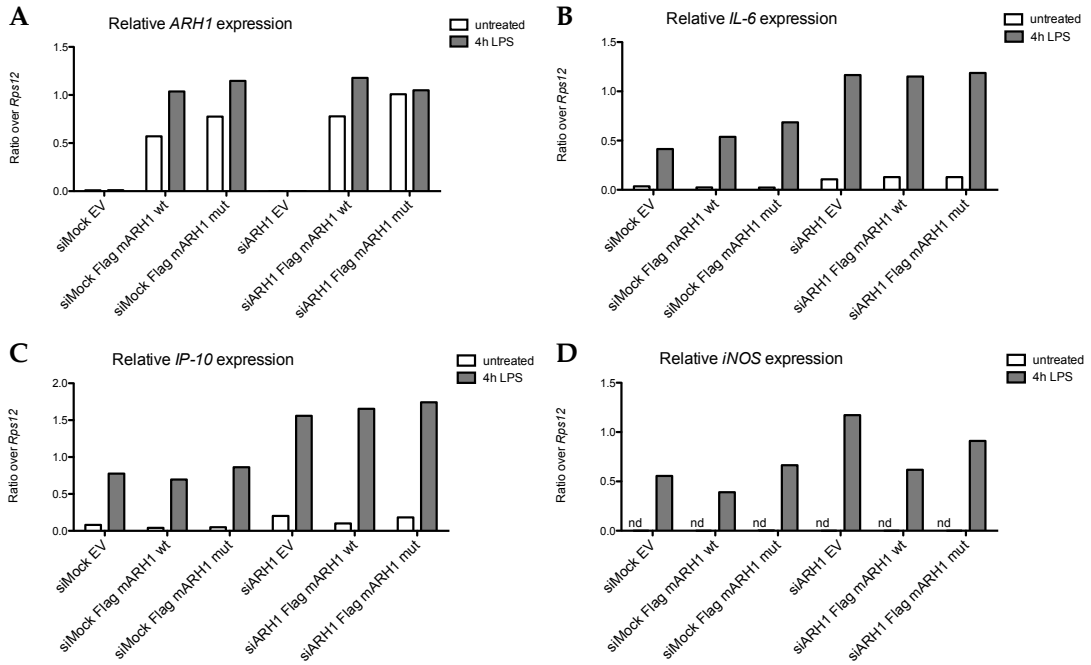

Figure 17: Overexpression of mARH1 wt but not mut decreases *iNOS* expression after 4 h LPS treatment in a siARH1 background. NIH3T3 cells treated with siMock or ARH1 and transfected with pcDNA3.1 empty vector, Flag-tagged mARH1 wt or Flag-tagged mARH1 mut were either untreated or treated with LPS for 4 h and subsequently the expression measured of *ARH1* (A), *IP-10* (B), *IL-6* (C) or *iNOS* (D). This experiment was performed twice.

7.6 LPS stimulation does not alter the localization of mARH1 and hARH1 wt and mut

To provide further insight into the molecular mechanism and in which compartment ARH1 regulates LPS induced *iNOS* expression, the localization of Flag-tagged mARH1 wt and mut upon LPS treatment was tested. NIH3T3 cells were transfected with calcium phosphate with Flag-tagged mARH1 wt or mut as well as pcDNA3.1 empty vector as control. After two days, cells were treated with LPS for 30 min, after which NF-κB is known to translocate to the nucleus. Cells were fixed with PFA and the immunofluorescence performed with the corresponding antibodies (anti-p65, anti-Flag) and DAPI by mounting with VECTASHIELD antifade mounting medium. Although NF-κB efficiently translocated to the nucleus upon LPS stimulation, Flag-tagged mARH1 wt and mut remained in the cytoplasm (Figure 18), suggesting that LPS does not alter the localization of mARH1 and that neither ARH1 wt nor mutant regulates the translocation of NF-κB.

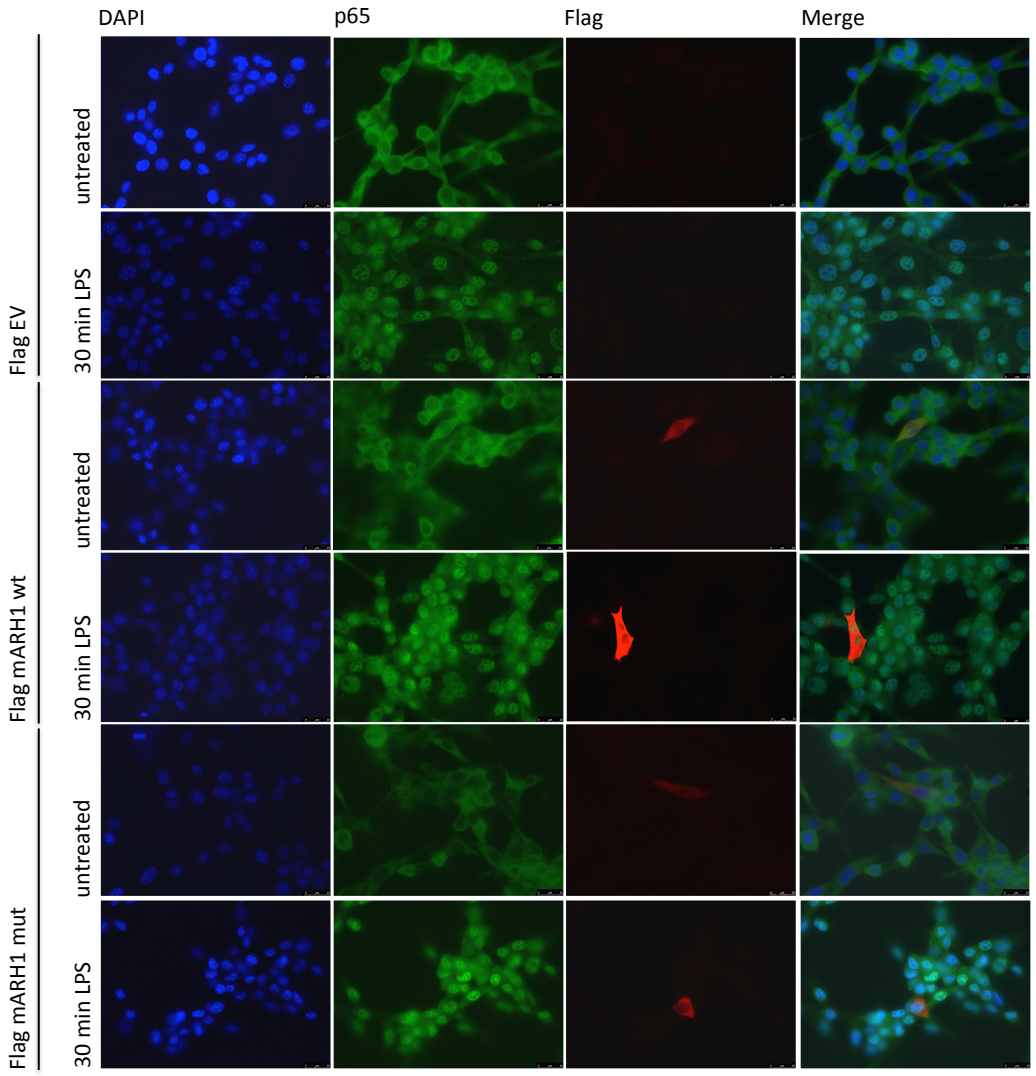

Figure 18: mARH1 wt and mut do not change their localization upon LPS treatment. NIH3T3 cells were transfected with Flag-tagged mARH1 wt, ARH1 mut or with pcDNA3.1 empty vector as control and treated for 30 min with LPS. Cells were stained with DAPI by mounting with VECTASHIELD antifade mounting medium (1st row), p65 (2nd row) or Flag to detect ARH1 (3rd row). The last row shows a merge of all three stainings. This is a representative example of two independent immunofluorescences.

To test whether the same holds true for the human counterpart, HEK TLR4 cells (HEK cells overexpressing TLR4 and thus responsive to LPS treatment) were transfected with calcium phopsphate using the Flag-tagged hARH1 wt, hARH1 mut expression vectors or pcDNA3.1 empty vector as control. After 2 days, cells were treated with LPS for 30 min, fixed with PFA and immunofluorescence was performed with the corresponding antibodies and DAPI by mounting with VECTASHIELD antifade mounting medium. Although NF-κB efficiently translocated after 30 min LPS stimulation to the nucleus also in these cells, Flag-tagged hARH1 wt and mut remained in the cytoplasm (Figure 19), suggesting that also in the human

system, LPS stimulation does not alter the localization of hARH1, and hARH1 does not directly affect the nuclear translocation of NF-κB.

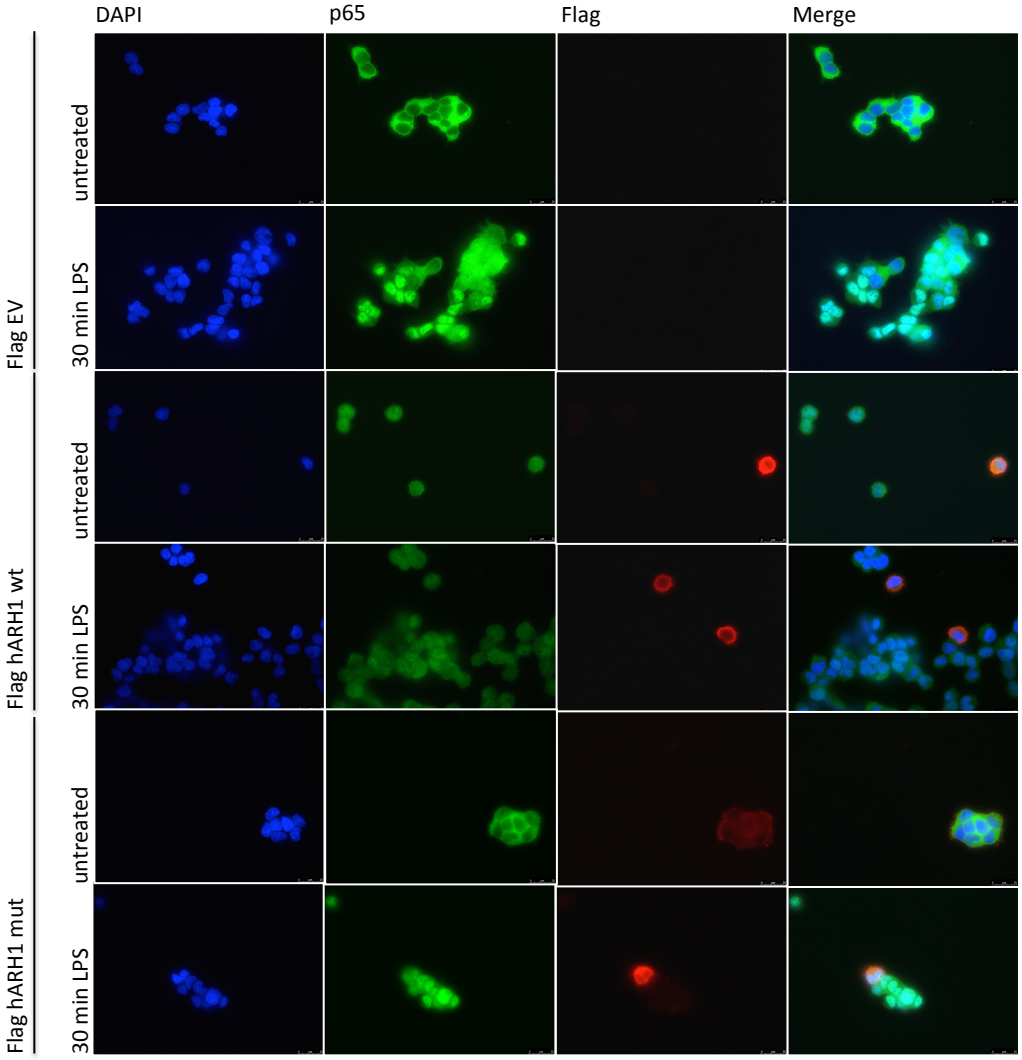

Figure 19: hARH1 wt and mut do not change their localization upon LPS treatment. HEK TLR4 cells were transfected with Flag-tagged hARH1 wt, hARH1 mut or with pcDNA3.1 empty vector as control and treated for 30 min with LPS. Cells were stained with DAPI by mounting with VECTASHIELD antifade mounting medium (1st row), p65 (2nd row) or Flag to detect hARH1 (3rd row). The last row shows a merge of all three stainings. This is a representative example of two independent immunofluorescences.

7.7 ARH1 regulates *iNOS* expression only after 4 h after LPS treatment

To functionally confirm that ARH1 does not affect the LPS-induced NF-κB-dependent gene expression in a direct manner, NIH3T3 cells were treated with siMock as control and siARH1 and further stimulated after 44 h for 1 or 4 h with LPS. RNA was subsequently isolated, reverse transcribed to cDNA and the expression of the same NF-κB target genes again quantified by qRT-PCR. The knockdown of *ARH1* was as efficient as observed in the other

experiments (Figure 20A). 1 h LPS treatment induced the expression of *IP-10* and *IL-6*, but not of *iNOS*, which agrees with both genes being early response genes (Figure 20B-D). Knockdown of ARH1 had only little effect at this time point. After 4 h of LPS treatment, the expression of *IP-10* and *IL*-6 already decreased, while the expression of *iNOS* was detectable only at this time point (Figure 20B-D). Again, knocking down ARH1 enhanced *iNOS* expression at this time point compared to the siMock sample (Figure 20D). Together these experiments suggested that ARH1 unlikely affects the LPS-induced nuclear translocation of NF-κB and the expression of the early response genes, but rather affected the late response genes such as *iNOS*, which is possibly induced by an LPS-induced secondary stimulus.

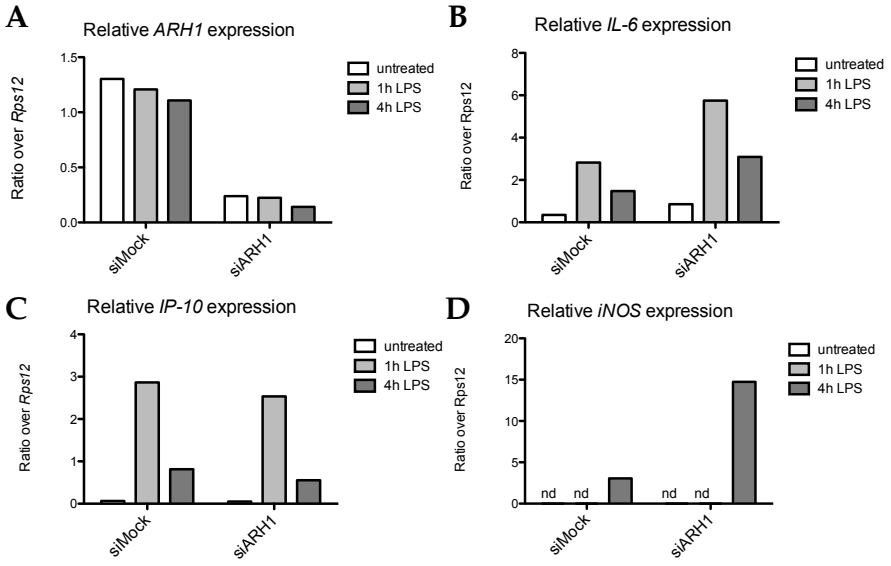

Figure 20: ARH1 knockdown only enhances *iNOS* expression after 4 h but not 1h LPS stimulation. NIH3T3 cells treated with siMock or siARH1 and stimulated for 1h LPS or 4 h LPS were analyzed for the relative expression of *ARH1* (A), *IL-6* (B) *IP-10* (C), or *iNOS* (D). The provided result is a representative example of 3 independently performed experiments.

To investigate whether the induction and expression of *iNOS* depends on the expression of another stimulus (i.e. in a second pathway), a LPS pulse treatment experiment was performed. NIH3T3 cells were treated with siMock as control or siARH1 for 48 h and subsequently pulse-treated with LPS for only 15 min, the medium exchanged and gene expression measured after additional 45 minutes or 3 h 45 min. The knockdown of *ARH1* was as efficient (Figure 21A). 45 min after pulse treatment, the expression of *IP-10*, but not of *iNOS* was induced (Figure 21C-D). Knockdown of ARH1 had no effect on the gene expression at this time point. 3 h 45 min after the LPS pulse treatment, the expression of *IP-10* already decreased, while the expression of *iNOS* was nicely detectable at this time point (Figure 21D). In contrast to earlier experiments with continuous LPS treatment, knockdown of ARH1

enhanced *iNOS* expression at this time point only slightly 1.5-fold compared to the siMock sample (Figure 21D), compared to 3-4 fold (Figure 20D), strongly arguing that *iNOS* expression is most likely induced by a LPS-induced stimulus which induces a secondary signaling pathway that is affected by ARH1.

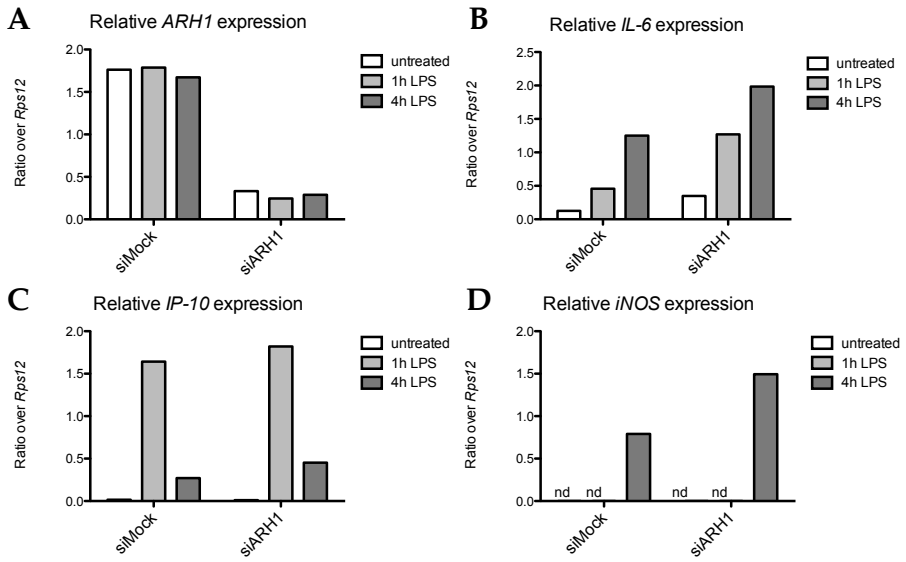

Figure 21: LPS pulse treatment reduces the effect of ARH1 knockdown on *iNOS* expression. Cells were transfected with siMock and siARH1 and treated for 1 and 4 h pulse treatment with LPS. Media was exchanged 15 min after adding LPS to the cells and the relative expression analyzed for *ARH1* (A), *IL-6* (B) *IP-10* (C) or *iNOS* (D). This is a representative example of two independent experiments.

7.8 *iNOS* expression is regulated by ARTD8

iNOS has been described to be also regulated by Stats beside NF-κB [55]. The iNOS promoter possesses binding sites for different Stats and Stat signaling can be activated by IL-6 [46, 60], which was found to be induced 1 h after LPS stimulation. The nuclear ARTD8 is the only mono-ADP-ribosyltransferase of the ARTD family member known to interact with Stats. To test whether ARTD8 is important for the expression of *iNOS*, NIH3T3 cells were treated with siMock, siARH1, siARTD8 and siARH1 together with siARTD8 to knockdown both proteins. 44 h after transfection, cells were treated with LPS for 4 h, RNA was isolated, reverse-transcribed to cDNA and gene expression quantified by qRT-PCR. An efficient knockdown for ARH1 as well as ARTD8 was observed under the tested conditions. 4 h LPS treatment induced *IP-10* and *iNOS*, and the single knockdown of ARH1 enhanced the expression of *iNOS* as already observed in earlier experiments (Figure 22D-E). The expression of *IκBα* was not enormously altered under the tested conditions (Figure 22F). Knockdown of ARTD8 alone reduced the LPS-induced expression of *IP-10* slightly and of

iNOS very strongly (Figure 22D-E), suggesting that ARTD8 is indeed required for the expression of these two genes. The expression of *IκBα* was not or only weakly affected by the reduction of ARTD8. Interestingly, when *ARH1* and *ARTD8* were together knocked down, the enhanced expression of *iNOS* and *IP-10* expression was abrogated (Figure 22D-E), suggesting that ARTD8 and ARH1 indeed functionally cooperate and that most likely the Stat signaling is important for the expression of *iNOS* at this time point of LPS stimulation.

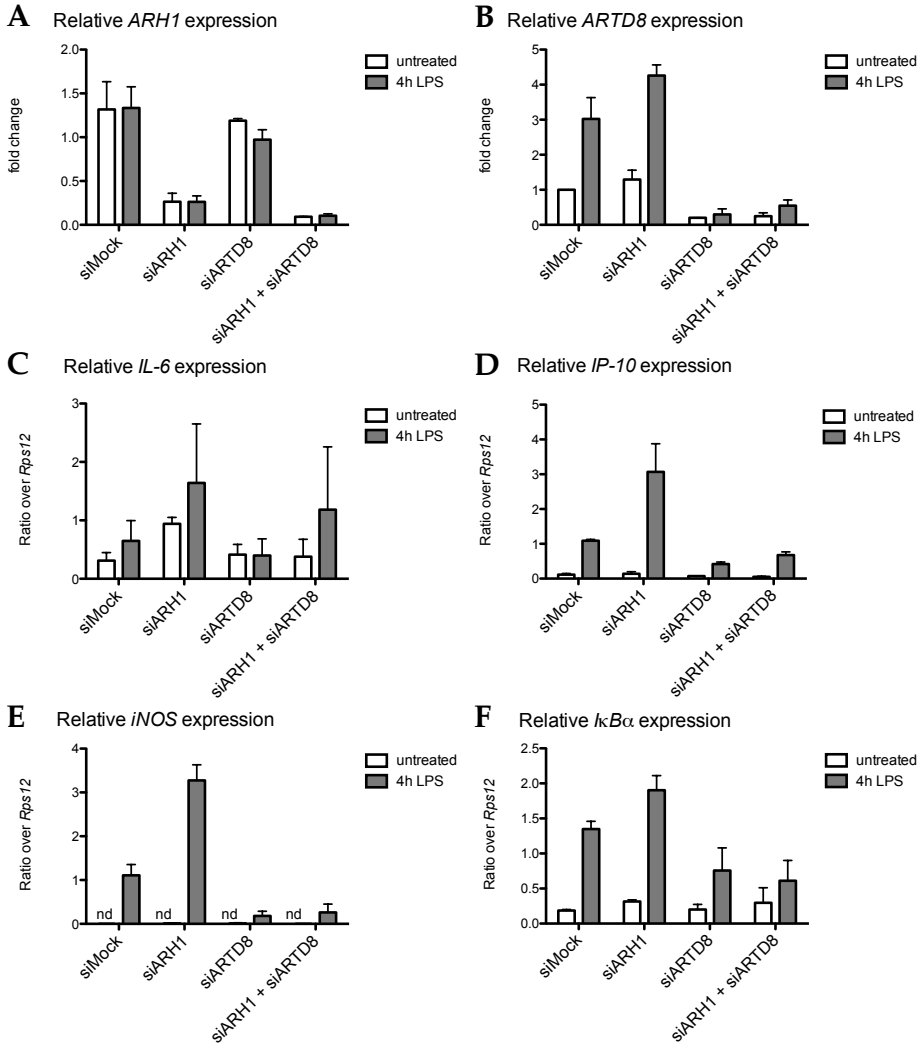

Figure 22: *iNOS* expression is regulated by ARTD8, which abrogates the siARH1 effect. Cells were transfected with siMock, siARH1, siARTD8 or siARH1 with siARTD8 and treated for 4 h with LPS. Relative expression was analyzed for *ARH1* (A), *ARTD8* (B), *IL-6* (C), *IP-10* (D), *iNOS* (E) or *IκBα* (F). This figure recapitulates 2 independently performed experiments.

7.9 Stat6 cooperates with ARH1 to regulate the *iNOS* expression

Since ARTD8 was described to be a co-factor of Stat6, the involvement of Stat6 in iNOS expression and a possible cross talk with ARH1 was analyzed. NIH3T3 cells were transfected

with siMock, siARH1, siStat6 or siARH1 together with siStat6 to knockdown both proteins. 44 h after transfection, cells were treated with LPS for 4 h, RNA was isolated, reverse-transcribed to cDNA and gene expression quantified by qRT-PCR. An efficient knockdown for ARH1 as well as Stat6 was observed under the tested conditions (Figure 23A-B). 4 h LPS treatment induced *IP-10* and *iNOS*, and the single knockdown of ARH1 enhanced the expression of *IP-10* and *iNOS* as already observed in earlier experiments (Figure 23D-E). The expression of *IκBα* was not enormously altered under the tested conditions (Figure 23F). Knockdown of Stat6 alone did not reduce the LPS induced expression of *IP-10* and *iNOS* (Figure 23D-E), suggesting that Stat6 is not required for the basal expression of these two genes. The expression of *IκBα* was not or only weakly affected by the reduction of Stat6. Interestingly, when *ARH1* and *Stat6* were knocked down together, the enhanced expression of *iNOS* and *IP-10* expression was again completely abrogated (Figure 23D-E), indicating that Stat6 and ARH1 indeed functionally cooperate in the regulation of *iNOS* expression 4 h after LPS stimulation.

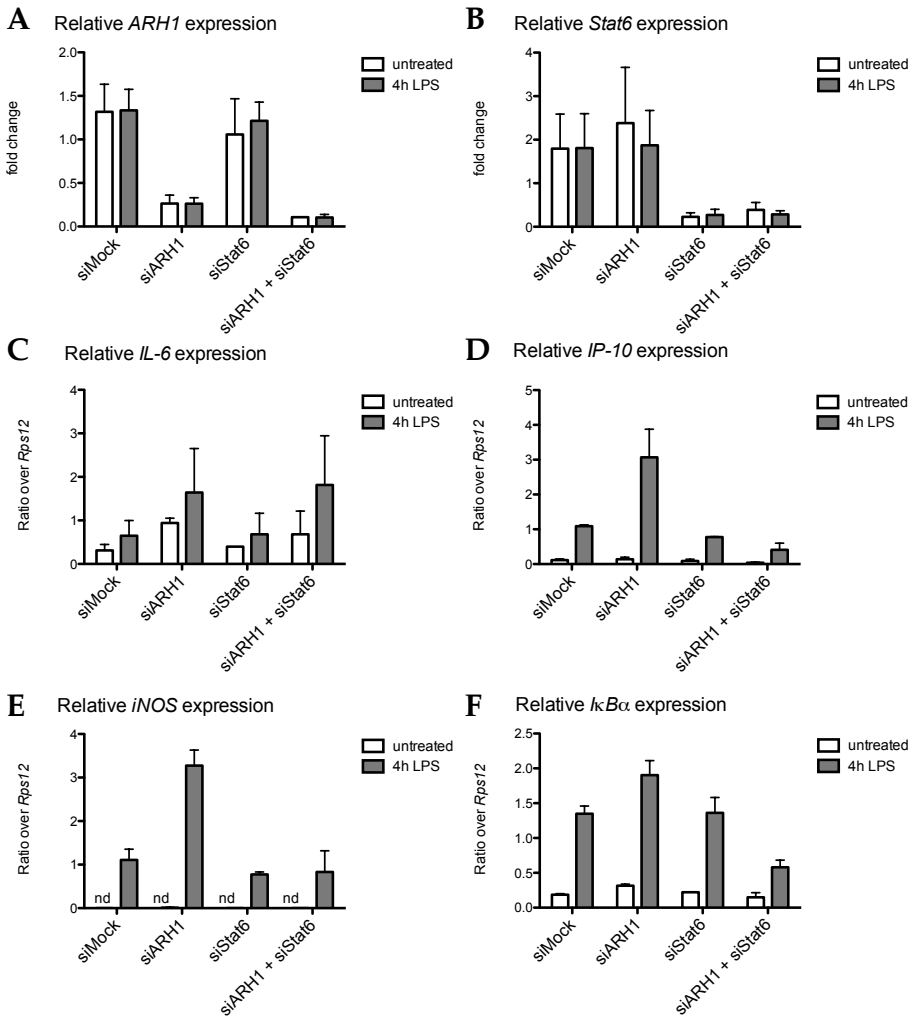

Figure 23: The dampening effect of siARH1 on *iNOS* expression is dependent on Stat6. Cells were transfected with siMock, siARH1, siStat6 or siARH1 with siStat6 and treated for 4 h with LPS. Relative expression was analyzed for *ARH1* (A), *ARTD8* (B), *IL-6* (C), *IP-10* (D), *iNOS* (E) or *IκBα* (F). This figure recapitulates 2 independently performed experiments.

7.10 LPS induces the nuclear translocation of Stat6

Stat6 was reported to translocate to the nucleus upon stimulation with IL-4 or IL-13 [46]. To investigate whether LPS would indirectly stimulate Stat6 nuclear translocation, immunofluorescence experiments were performed using an antibody against Stat6. NIH3T3 cells were either untreated or treated for 1 h, 2 h, 4 h with LPS, fixed with PFA and immunofluorescence performed.

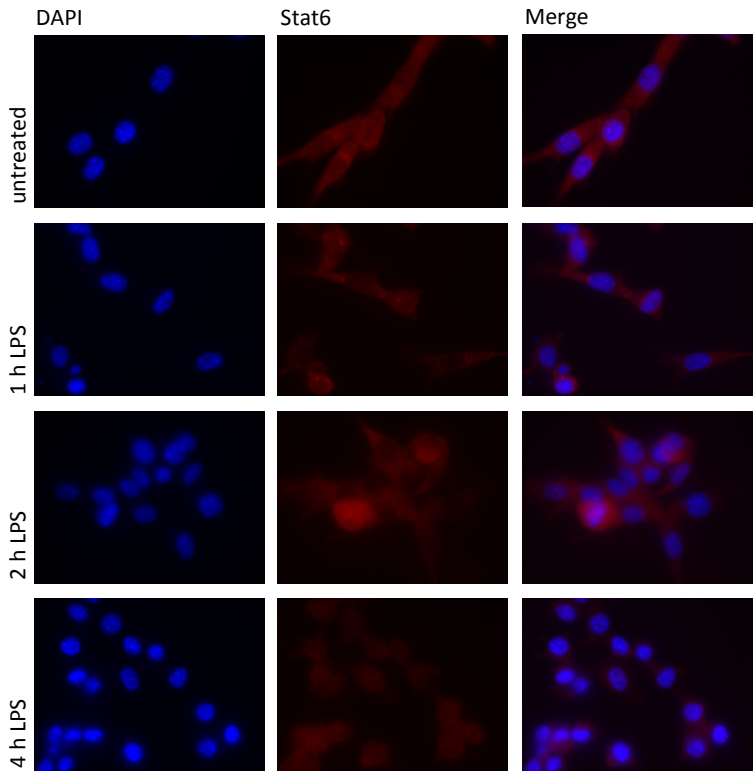

Figure 24: LPS induces the nuclear translocation of Stat6. NIH3T3 cells were stimulated for 1 h, 2 h and 4 h with LPS. Cells were stained with DAPI by mounting with VECTASHIELD antifade mounting medium and with anti-Stat6. The last row shows a merge of all three stainings. This is a representative example of to independent immunofluorescences.

Under untreated conditions, Stat6 staining was cytoplasmic, as expected, and did not overlap with DAPI staining. After 1 h or 2 h LPS stimulation, the observed cytoplasmic localization of Stat 6 became diffuse, while after 4 h LPS treatment Stat6 staining overlapped with the DAPI staining (Figure 24), indicating that at this time point, LPS is able to induce the nuclear translocation of Stat6.

7.11 The enzymatic activity of ARH1 is not required for the LPS induced nuclear translocation of Stat6

Based on the results obtained so far, ARH1 might affect the expression of iNOS by interfering with the translocation of Stat6. To investigate the influence of ARH1 and its enzymatic activity on the translocation of Stat6 after 4 h LPS treatment, NIH3T3 cells were transfected with calcium phosphate with Flag-tagged mARH1 wt, Flag-tagged mARH1 mut or pcDNA3.1 empty vector as control. 44 h after transfection, cells were treated with LPS for 4 h. After the treatment, NIH3T3 cells were fixed with PFA and immunofluorescence performed with antibodies against Stat6 and Flag (Figure 25).

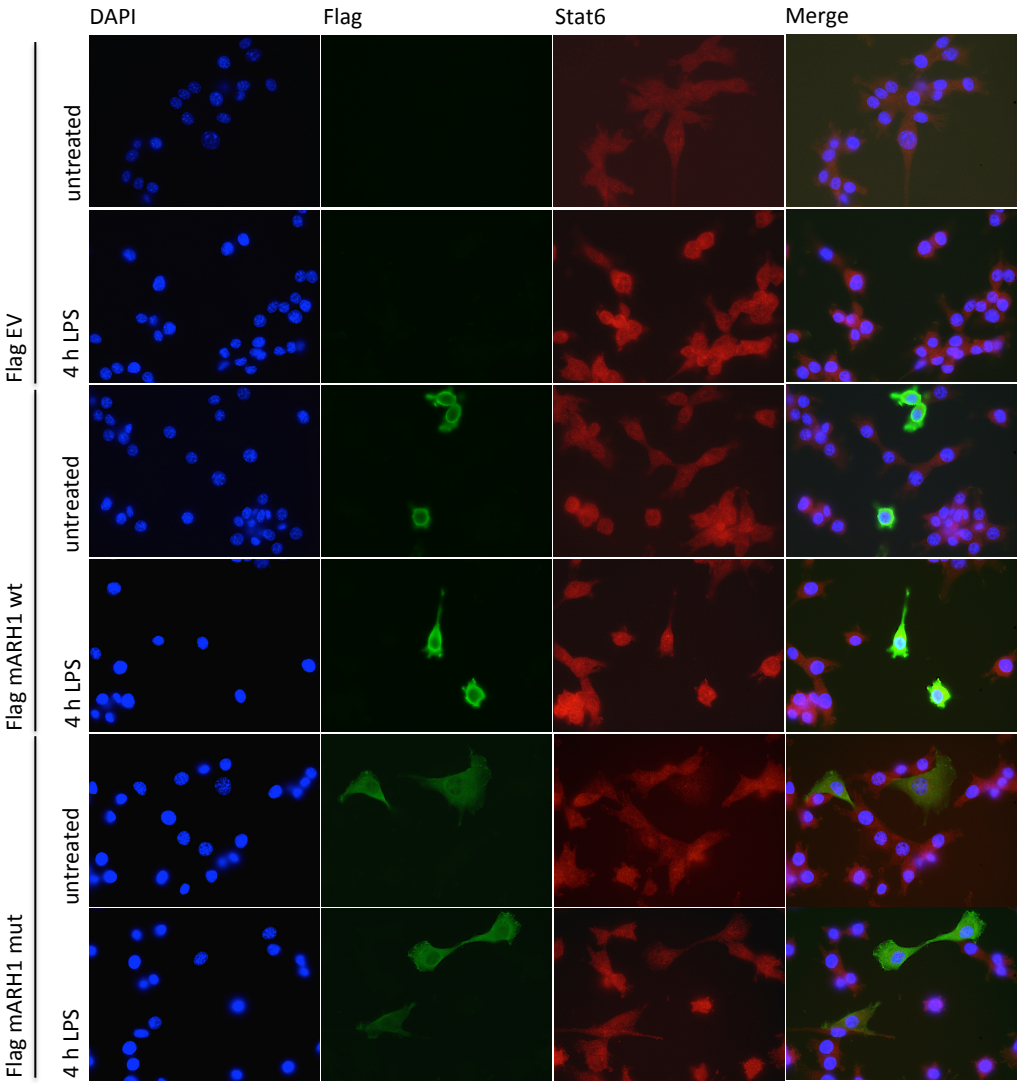

Figure 25: Overexpression of mARH1 mut but not mARH1 wt dampens the LPS induced nuclear translocation of Stat6. NIH3T3 cells were transfected with Flag-tagged mARH1 wt or mut and stimulated after 44 h for 4 h with LPS. Cells were stained with DAPI by mounting with VECTASHIELD antifade mounting medium (1st row), Flag to detect ARH1 (2nd row) or Stat 6 (3rd row). The last row shows a merge of all three staining. This is a representative example of two independent immunofluorescences.

Nuclear translocation of Stat6 was observed upon LPS treatment when mARH1 wt, mARH1 mut or the pcDNA3.1 empty vector where transfected (Figure 25).

8 Discussion

ADP-ribosylation has been implicated in different distinct cellular and biological processes through controlling the function of modified proteins [61]. Some ARTDs (e.g. ARTD1, ARTD8, ARTD9, ARTD10, ARTD12) are known to be involved in inflammation, suggesting that also mono-ADP-ribosyhydrolases, such as ARH1, which is already known to have an influence on cancer development, may co-regulate inflammation [31, 32].

In this thesis, we thus elucidated the role and the molecular mechanisms of the mono-ADP-ribosylhydrolase ARH1 during LPS-induced pro-inflammatory signaling. We show that knockdown of ARH1 enhances the expression of the inflammatory genes *iNOS* and *IP-10*, suggesting that ARH1 usually has a dampening effect on the expression of these genes. Other genes, such as *IL-6* or *IκBα,* were not affected by knockdown of ARH1 under the tested conditions. Furthermore, we confirmed that the enzymatic activity of ARH1 is important for the observed effect, suggesting that mono-ADP-ribosylation is involved in the regulation of LPS-induced signaling events. Immunofluorescence experiments demonstrated that NF-κB translocates to the nucleus in ARH1 overexpressing cells after 30 min of LPS treatment, very similar to non-transfected cells, indicating that ARH1 does not interfere with the nuclear translocation of NF-κB. We further have provided evidence that ARH1 does not directly regulate the LPS-induced NF-κB pathway by performing an LPS stimulation time course experiment. The enhancing effect of ARH1 knockdown on *iNOS* and *IP-10* was only observed after 4 h and not 1 h of LPS treatment. In search for other pro-inflammatory signaling pathways that may regulate *iNOS* expression, a functional crosstalk between ARH1 and ARTD8, a co-factor of Stat6 [50], was tested. Surprisingly, knockdown of ARTD8 completely abrogated *iNOS* and *IP-10* upregulation upon LPS stimulation, suggesting that ARTD8 is required for the expression of these genes. In addition, the observed upregulation of *iNOS* and *IP-10* upon knockdown of ARH1 was reversed when ARTD8 was also knocked down. When knocking down Stat6, only the effect of ARH1 knockdown could be reversed, while the LPS-induced expression of *iNOS* and *IP-10* was not affected, suggesting that other Stats (e.g. Stat1 and/or Stat3) could regulate the LPS-induced *iNOS* expression. Finally, we have provided preliminary evidence for the nuclear translocation of Stat6 upon 4 h LPS stimulation by immunofluorescence, linking Stat6 nuclear translocation to *iNOS* expression

and suggesting that ARH1 might indeed regulate *iNOS* expression through Stat6 and ARTD8 [46].

The fact that only the expression of *iNOS* (and to a lesser extent that of *IP-10*), but not of *IL-6* or *IκBα* was affected, could be due to different chromatin states at the respective promoter regions. Moreover, different transcription factors in addition to NF-κB might regulate the respective gene. Our data suggest that ARTD8 functions as transcription co-factor of Stat hetero- or homodimers (e.g. Stat1/3) once bound to the DNA, since knockdown of ARTD8, a known Stat6 co-factor, not only prevents the effect of ARH1 knockdown on *iNOS* expression, but the overall LPS-induced gene expression of *iNOS*. This is in contrast to what is already known about ARTD8, namely that it binds to Stat6-responsive promoters and exhibits specific binding to the DNA it is associated with, thereby enhancing IL-4 and Stat6 function [50] [62].

The *iNOS* expression seems to be induced only after 4 h of LPS stimulation and not to be dependent on the nuclear translocation of NF-κB after 30 minutes, suggesting that possibly one of the immediate early NF-κB target genes would be translated and further activate Stat signaling in an autocrine manner. IL-6 would be a strong candidate, as it is already known to activate Stat signaling (Stat1 and Stat3) [45]. Based on our data, we would further speculate that ARH1 mainly affects the secondary signaling through crosstalk with Stat6 in the cytoplasm, since the initial nuclear translocation of NF-κB, as well as the expression of other immediate early genes, were not affected.

The fact that the enzymatic activity of ARH1 is involved in the regulation of *iNOS* expression, and that the ARH1 effect was completely dependent on Stat6, suggests that a cytoplasmically located ARTD family member presumably modifies Stat6 or a protein X bound to Stat6 either as a consequence of LPS and/or LPS/IL-6 stimulation or even under basal conditions. It is plausible to assume that Stats in general, and specifically Stat6 in this case, is ADP-ribosylated, since Stats are generally known to be extensively post-translationally modified [45, 63]. Which ARTD family member mediates this putative modification remains to be elucidated (Table 1). ARTD8 is very unlikely the modifying enzyme, since it is localized in the nucleus and seems to affect Stat signaling only in the nuclear compartment [50]. Besides ARTD8, no other ARTD family member is yet known to interact with Stats. However, ARTD10 has recently been described to influence TNFα-induced singling [12]. One could speculate that a member of the ARTC family member, known to modify proteins at arginine residues, might be responsible for the modification of

Stat6/protein X, although they would have to enter the cell or change their cellular localization to do so. Alternatively, protein X might be an extracellular factor that gets modified upon LPS stimulation and enters the cell to form a complex with Stat6.

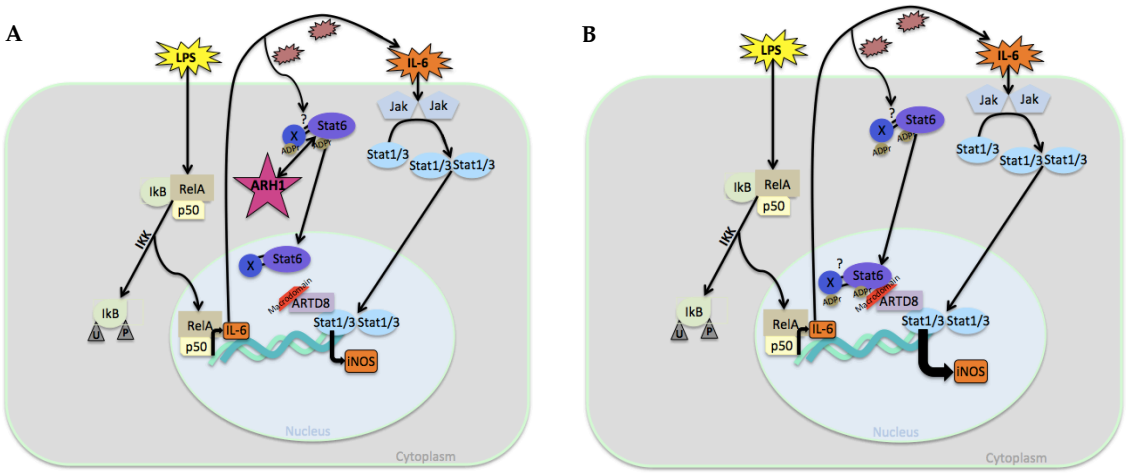

Figure 26: Model of ARH1 as suppressor of LPS-induced pro-inflammatory signaling. Two scenarios for ARH1 proficient (A) or deficient condition (B).

Our data provide evidence for a model in which ARH1 is a suppressor of certain LPS-induced NF-κB target genes by interacting with Stat6 directly or through a protein X (Figure 26A).

In this model, NF-κB signaling is induced upon LPS treatment and activates target gene expression such as *iNOS*, *IL*-6, *IP*-10 and *IκB*. Upon stimulation of cells with LPS for several hours, *IL-6* upregulation and expression could potentially activate Stat1 and/or Stat3 and thereby enhance gene expression of *iNOS,* which is known to have binding sites for Stat1 and Stat3 in its promoter region [64]. However, at this moment, we can not exclude that other cytokines may (also) induce Stat signaling and *iNOS* expression (e.g. IFNγ). Since the enzymatic activity of ARH1 is involved in the functional crosstalk of ARTD8/Stat6 signaling, we speculate that ARH1 might hydrolyze the mono-ADP-ribosylation of either Stat6 or the yet undiscovered protein X, which forms a complex with Stat6. ADP-ribosylation of Stat6 or protein X seems to enhance *iNOS* expression, since knockdown of ARH1 or overexpression of the ARH1 enzymatically inactive mutant both enhanced *iNOS* expression (Figure 26B). The ADP-ribosylation of Stat6 or protein X most likely changes the physical properties of the protein or allows interaction with another protein containing an ADP-ribosylation binding domain. Along this line, we speculate that under physiological conditions, in the presence of ARH1 and demodification of Stat6/protein X, the de-modified Stat6/protein X is still able to

translocate to the nucleus, but not able to bind proteins recruited to the chromatin such as ARTD8 which contains macrodomains (i.e. ADP-ribosylation binding domains). ARTD8 is most likely recruited as co-factor of Stat1 or Stat3, which results in moderate *iNOS* gene transcription. In contrast, when ARH1 is missing and its enzymatic activity does not reverse ADP-ribosylation of Stat6/protein X, the complex translocates to the nucleus where it could be bound by the ARTD8 macrodomain. This would allow Stat6 to form a ARTD8-mediated complex with other transcription factors (Stat1 or Stat3) localized at the promoter region of *iNOS,* and thereby enhance LPS-induced *iNOS* and *IP-10* expression (Fig. 26B).

Whether these findings are medically relevant has to be further investigated. NO produced by NOS, has been found to be involved in inflammation controlling infection, regulating signaling cascades and transcription factors, and regulating leukocyte rolling, migration, cytokine production, proliferation and apoptosis. Inhibitors of NO synthesis, especially selective iNOS inhibitors have been shown to be anti-inflammatory in various forms of experimentally induced inflammation [65]. Additionally, iNOS generates more NO than the constitutive members nNOS or eNOS, and is expressed after cytokine exposure, and more specifically modulates important tumor related processes such as malignant transformation, angiogenesis, and metastasis [66]. The observed effect of ARH1 on *iNOS* expression, and the subsequent dampening of the inflammatory response, might thus indirectly contribute to the described tumor suppressor function of ARH1 in cancer development [31, 32].

To date, Stat6 has been reported to play a distinct role in T-cell development and IFNγ signaling important for the immune system [52]. Together with Stat4, Stat6 plays an important role in controlling cell-cycle progression and apoptosis and thus contributes to oncogenesis. Linking Stat6 to the expression of *iNOS* is an important aspect, because by inhibiting Stat6, the inflammatory signaling or tumorigenesis could be limited.

Additional experiments are required to further develop and fully confirm the current model. To define which LPS-induced factor is responsible for the induction of *iNOS*, the involvement of IL-6 or another LPS-induced Stat inducer should be proven by performing knockdown experiments in the absence or presence of ARH1 and subsequent analysis of the *iNOS* expression. If the knockdown of *IL-6* would counteract the observed dampening effect of ARH1 on *iNOS* expression or the general *iNOS* induction, the link to IL-6 would be confirmed. Additionally, the induction of Stat1/Stat3 signaling by IL-6 could be tested by stimulating NIH3T3 cells directly with IL-6 in the presence or absence of LPS. An effect on

iNOS and *IP-10* upon ARH1 knockdown in these experiments would be expected at an earlier time point than 4 h due to the direct signaling.

To investigate whether Stat1 and/or Stat3 are indeed responsible for the LPS induced *iNOS* expression, a knockdown of Stat1/Stat3 should be performed. If Stat1/Stat3 is responsible for enhanced *iNOS* expression, we speculate that *iNOS* expression will no longer be upregulated in cells with a knockdown of the responsible Stat.

Furthermore, to find possible candidates that might be demodified by ARH1 upon LPS stimulation, immunoprecipitation of ARH1 after 4 h LPS treatment should be performed. Interactors could be identified by mass spectrometry. To enhance a possible interaction, the experiments could be performed upon overexpression of an enzymatically inactive ARH1mutant. The direct interaction with such candidates could subsequently be confirmed *in vitro*.

Before ARH1 can ultimately be proven as ADP-ribosylhydrolase of a target protein involved in inflammatory signaling, the responsible writer for the modification of Stat6/protein X has still to be identified. Therefore, different ARTDs family members could be knocked down and the expression of *iNOS* reanalyzed after LPS stimulation. Interesting candidates might subsequently be overexpressed and immunoprecipitated from cells. By using these ARTDs in *in vitro* assays together with potential ARH1 target proteins, the right ARTD family member(s) might be identified. In addition, such experiments could be linked to de-modification experiments using ARH1.

In order to detect whether Stat6 is really ADP-ribosylated, an anti-Stat6 immunoprecipitation of a whole cell extract should be performed and analyzed by mass spectrometry [67]. These experiments will not only confirm that Stat6 is modified, but also indicate which amino acid is modified. The identified amino acid could subsequently by mutated and upon purification of recombinant proteins (wt and modification-deficient mut) be confirmed *in vitro* using potential writers (see above).

The complex formation of Stat6 with ARTD8 has already been reported [62]. To confirm that the reported complex formation of Stat6 with A[30]RTD8 is mediated by ADP-ribosylation [62], immunoprecipitation experiment should be performed using cells treated with ADP-ribosylation inhibitors (e.g. PJ34, ABT888). If the interaction is due to ADP-ribosylation, ARTD8 will not co-immunoprecipitate with Stat6. To show that the macrodomain of ARTD8 is responsible for binding to ADP-ribosylated Stat6, co-

immunoprecipitation experiments with a mutant of ARTD8 lacking the macrodomain could be performed.

Together, we provide strong evidence that ARH1 and its enzymatic activity is involved in LPS-induced pro-inflammatory signaling and particularly the expression of *iNOS* and *IP-10*. ARH1 dampened the gene expression of *iNOS* and *IP-10*. Furthermore, we have shown that the ARH1-mediated effect is dependent on Stat6 and that nuclear ARTD8 contributes to this effect.

9 References

1. Hottiger, M.O., *Nuclear ADP-Ribosylation and Its Role in Chromatin Plasticity, Cell Differentiation, and Epigenetics*. Annu Rev Biochem, 2015. **84**: p. 227-63.
2. Hottiger, M.O., *SnapShot: ADP-Ribosylation Signaling*. Mol Cell, 2015. **58**(6): p. 1134-1134 e1.
3. Moss, J., M.K. Jacobson, and S.J. Stanley, *Reversibility of arginine-specific mono(ADP-ribosyl)ation: identification in erythrocytes of an ADP-ribose-L-arginine cleavage enzyme*. Proc Natl Acad Sci U S A, 1985. **82**(17): p. 5603-7.
4. Oka, S., J. Kato, and J. Moss, *Identification and characterization of a mammalian 39-kDa poly(ADP-ribose) glycohydrolase*. J Biol Chem, 2006. **281**(2): p. 705-13.
5. Alvarez-Gonzalez, R. and H. Mendoza-Alvarez, *Dissection of ADP-ribose polymer synthesis into individual steps of initiation, elongation, and branching*. Biochimie, 1995. **77**(6): p. 403-7.
6. Wielckens, K., et al., *Protein-bound polymeric and monomeric ADP-ribose residues in hepatic tissues. Comparative analyses using a new procedure for the quantification of poly(ADP-ribose)*. Eur J Biochem, 1981. **117**(1): p. 69-74.
7. Wielckens, K., et al., *DNA fragmentation and NAD depletion. Their relation to the turnover of endogenous mono(ADP-ribosyl) and poly(ADP-ribosyl) proteins*. J Biol Chem, 1982. **257**(21): p. 12872-7.
8. Haag, F. and F. Buck, *Identification and analysis of ADP-ribosylated proteins*. Curr Top Microbiol Immunol, 2015. **384**: p. 33-50.
9. Schreiber, V., et al., *Poly(ADP-ribose): novel functions for an old molecule*. Nat Rev Mol Cell Biol, 2006. **7**(7): p. 517-28.
10. Naia, L. and A.C. Rego, *Sirtuins: double players in Huntington's disease*. Biochim Biophys Acta, 2015. **1852**(10 Pt A): p. 2183-94.
11. Rosenthal, F. and M.O. Hottiger, *Identification of ADP-ribosylated peptides and ADP-ribose acceptor sites*. Front Biosci (Landmark Ed), 2014. **19**: p. 1041-56.
12. Feijs, K.L., P. Verheugd, and B. Luscher, *Expanding functions of intracellular resident mono-ADP-ribosylation in cell physiology*. FEBS J, 2013. **280**(15): p. 3519-29.
13. Altmeyer, M., et al., *Molecular mechanism of poly(ADP-ribosyl)ation by PARP1 and identification of lysine residues as ADP-ribose acceptor sites*. Nucleic Acids Res, 2009. **37**(11): p. 3723-38.
14. Seman, M., et al., *Ecto-ADP-ribosyltransferases (ARTs): emerging actors in cell communication and signaling*. Curr Med Chem, 2004. **11**(7): p. 857-72.
15. Mashimo, M., J. Kato, and J. Moss, *Structure and function of the ARH family of ADP-ribosyl-acceptor hydrolases*. DNA Repair (Amst), 2014. **23**: p. 88-94.
16. Rosenthal, F., et al., *Macrodomain-containing proteins are new mono-ADP-ribosylhydrolases*. Nat Struct Mol Biol, 2013. **20**(4): p. 502-7.
17. Koch-Nolte, F., et al., *Mammalian ADP-ribosyltransferases and ADP-ribosylhydrolases*. Front Biosci, 2008. **13**: p. 6716-29.

18. Li, N. and J. Chen, *ADP-ribosylation: activation, recognition, and removal*. Mol Cells, 2014. **37**(1): p. 9-16.
19. Virag, L., et al., *Poly(ADP-ribose) signaling in cell death*. Mol Aspects Med, 2013. **34**(6): p. 1153-67.
20. Sonnenblick, A., et al., *An update on PARP inhibitors--moving to the adjuvant setting*. Nat Rev Clin Oncol, 2015. **12**(1): p. 27-41.
21. Karlberg, T., et al., *Structural biology of the writers, readers, and erasers in mono- and poly(ADP-ribose) mediated signaling*. Mol Aspects Med, 2013. **34**(6): p. 1088-108.
22. Mortusewicz, O., et al., *Feedback-regulated poly(ADP-ribosyl)ation by PARP-1 is required for rapid response to DNA damage in living cells*. Nucleic Acids Res, 2007. **35**(22): p. 7665-75.
23. Giansanti, V., et al., *PARP inhibitors: new tools to protect from inflammation*. Biochem Pharmacol, 2010. **80**(12): p. 1869-77.
24. Rosado, M.M., et al., *Beyond DNA repair, the immunological role of PARP-1 and its siblings*. Immunology, 2013. **139**(4): p. 428-37.
25. Erener, S., et al., *Inflammasome-activated caspase 7 cleaves PARP1 to enhance the expression of a subset of NF-kappaB target genes*. Mol Cell, 2012. **46**(2): p. 200-11.
26. Butepage, M., et al., *Intracellular Mono-ADP-Ribosylation in Signaling and Disease*. Cells, 2015. **4**(4): p. 569-95.
27. Kaufmann, M., K.L. Feijs, and B. Luscher, *Function and regulation of the mono-ADP-ribosyltransferase ARTD10*. Curr Top Microbiol Immunol, 2015. **384**: p. 167-88.
28. Aguiar, R.C., et al., *B-aggressive lymphoma family proteins have unique domains that modulate transcription and exhibit poly(ADP-ribose) polymerase activity*. J Biol Chem, 2005. **280**(40): p. 33756-65.
29. Camicia, R., et al., *BAL1/ARTD9 represses the anti-proliferative and pro-apoptotic IFNgamma-STAT1-IRF1-p53 axis in diffuse large B-cell lymphoma*. J Cell Sci, 2013. **126**(Pt 9): p. 1969-80.
30. Wahlberg, E., et al., *Family-wide chemical profiling and structural analysis of PARP and tankyrase inhibitors*. Nat Biotechnol, 2012. **30**(3): p. 283-8.
31. Kato, J., et al., *ADP-ribosylarginine hydrolase regulates cell proliferation and tumorigenesis*. Cancer Res, 2011. **71**(15): p. 5327-35.
32. Kato, J., et al., *Mutations of the functional ARH1 allele in tumors from ARH1 heterozygous mice and cells affect ARH1 catalytic activity, cell proliferation and tumorigenesis*. Oncogenesis, 2015. **4**: p. e151.
33. Oeckinghaus, A., M.S. Hayden, and S. Ghosh, *Crosstalk in NF-kappaB signaling pathways*. Nat Immunol, 2011. **12**(8): p. 695-708.
34. Jost, P.J. and J. Ruland, *Aberrant NF-kappaB signaling in lymphoma: mechanisms, consequences, and therapeutic implications*. Blood, 2007. **109**(7): p. 2700-7.
35. Hayden, M.S. and S. Ghosh, *Signaling to NF-kappaB*. Genes Dev, 2004. **18**(18): p. 2195-224.
36. Hayden, M.S. and S. Ghosh, *NF-kappaB, the first quarter-century: remarkable progress and outstanding questions*. Genes Dev, 2012. **26**(3): p. 203-34.

37. Oeckinghaus, A. and S. Ghosh, *The NF-kappaB family of transcription factors and its regulation*. Cold Spring Harb Perspect Biol, 2009. **1**(4): p. a000034.
38. Pahl, H.L., *Activators and target genes of Rel/NF- κB transcription factors*. Oncogene, 1999. **18**.
39. Gerondakis, S., et al., *NF-kappaB control of T cell development*. Nat Immunol, 2014. **15**(1): p. 15-25.
40. Sun, S.C., *The noncanonical NF-kappaB pathway*. Immunol Rev, 2012. **246**(1): p. 125-40.
41. Neurath, M.F., et al., *Cytokine gene transcription by NF-kappa B family members in patients with inflammatory bowel disease*. Ann N Y Acad Sci, 1998. **859**: p. 149-59.
42. Feldmann, M., *The cytokine network in rheumatoid arthritis: definition of TNF alpha as a therapeutic target*. J R Coll Physicians Lond, 1996. **30**(6): p. 560-70.
43. Yamamoto, Y. and R.B. Gaynor, *Role of the NF-kappaB pathway in the pathogenesis of human disease states*. Curr Mol Med, 2001. **1**(3): p. 287-96.
44. Mantovani, A., *Molecular pathways linking inflammation and cancer*. Curr Mol Med, 2010. **10**(4): p. 369-73.
45. Delgoffe, G.M. and D.A. Vignali, *STAT heterodimers in immunity: A mixed message or a unique signal?* JAKSTAT, 2013. **2**(1): p. e23060.
46. Abroun, S., et al., *STATs: An Old Story, Yet Mesmerizing*. Cell J, 2015. **17**(3): p. 395-411.
47. Goenka, S. and M.H. Kaplan, *Transcriptional regulation by STAT6*. Immunol Res, 2011. **50**(1): p. 87-96.
48. Shuai, K. and B. Liu, *Regulation of JAK-STAT signalling in the immune system*. Nat Rev Immunol, 2003. **3**(11): p. 900-11.
49. Hebenstreit, D., et al., *Signaling mechanisms, interaction partners, and target genes of STAT6*. Cytokine Growth Factor Rev, 2006. **17**(3): p. 173-88.
50. Mehrotra, P., et al., *PARP-14 functions as a transcriptional switch for Stat6-dependent gene activation*. J Biol Chem, 2011. **286**(3): p. 1767-76.
51. Hoshino, A., et al., *STAT6-mediated signaling in Th2-dependent allergic asthma: critical role for the development of eosinophilia, airway hyper-responsiveness and mucus hypersecretion, distinct from its role in Th2 differentiation*. Int Immunol, 2004. **16**(10): p. 1497-505.
52. Pernis, A.B. and P.B. Rothman, *JAK-STAT signaling in asthma*. J Clin Invest, 2002. **109**(10): p. 1279-83.
53. Tomita, K., et al., *STAT6 expression in T cells, alveolar macrophages and bronchial biopsies of normal and asthmatic subjects*. J Inflamm (Lond), 2012. **9**: p. 5.
54. Demicco, E.G., et al., *Extensive survey of STAT6 expression in a large series of mesenchymal tumors*. Am J Clin Pathol, 2015. **143**(5): p. 672-82.
55. Aktan, F., *iNOS-mediated nitric oxide production and its regulation*. Life Sci, 2004. **75**(6): p. 639-53.
56. Mattila, J.T. and A.C. Thomas, *Nitric oxide synthase: non-canonical expression patterns*. Front Immunol, 2014. **5**: p. 478.
57. Simon, P.S., et al., *The NF-kappaB p65 and p50 homodimer cooperate with IRF8 to activate iNOS transcription*. BMC Cancer, 2015. **15**: p. 770.

58. Guo, F.H., et al., *Interferon gamma and interleukin 4 stimulate prolonged expression of inducible nitric oxide synthase in human airway epithelium through synthesis of soluble mediators*. J Clin Invest, 1997. **100**(4): p. 829-38.

59. Gulke, I., et al., *Characterization of the enzymatic component of the ADP-ribosyltransferase toxin CDTa from Clostridium difficile*. Infect Immun, 2001. **69**(10): p. 6004-11.

60. Jacobs, A.T. and L.J. Ignarro, *Cell density-enhanced expression of inducible nitric oxide synthase in murine macrophages mediated by interferon-beta*. Nitric Oxide, 2003. **8**(4): p. 222-30.

61. Scarpa, E.S., G. Fabrizio, and M. Di Girolamo, *A role of intracellular mono-ADP-ribosylation in cancer biology*. FEBS J, 2013. **280**(15): p. 3551-62.

62. Goenka, S. and M. Boothby, *Selective potentiation of Stat-dependent gene expression by collaborator of Stat6 (CoaSt6), a transcriptional cofactor*. Proc Natl Acad Sci U S A, 2006. **103**(11): p. 4210-5.

63. Ginter, T., T. Heinzel, and O.H. Kramer, *Acetylation of endogenous STAT proteins*. Methods Mol Biol, 2013. **967**: p. 167-78.

64. Calo, V., et al., *STAT proteins: from normal control of cellular events to tumorigenesis*. J Cell Physiol, 2003. **197**(2): p. 157-68.

65. Korhonen, R., et al., *Nitric oxide production and signaling in inflammation*. Curr Drug Targets Inflamm Allergy, 2005. **4**(4): p. 471-9.

66. Vannini, F., K. Kashfi, and N. Nath, *The dual role of iNOS in cancer*. Redox Biol, 2015. **6**: p. 334-43.

67. Rosenthal, F., et al., *Optimization of LTQ-Orbitrap Mass Spectrometer Parameters for the Identification of ADP-Ribosylation Sites*. J Proteome Res, 2015. **14**(9): p. 4072-9.

10 Acknowledgements

I am very thankful to everyone who helped and supported me during my studies and while working on this Doctoral thesis.

I want to thank Prof. Dr. Dr. Michael O. Hottiger for giving me the opportunity to work in his group and to perform this work.

I would also like to thank Prof. Dr. Hanspeter Nägeli for agreeing to review my thesis.

I am grateful to Jeannette Abplanalp and Michael O. Hottiger (both Department of Molecular Mechanisms of Disease, University of Zurich) for their helpful input during the planning and performing of the experiments.

Further, Jeannette Abplanalp is acknowledged for cloning hARH1 constructs into bacterial expression vectors. Joel Moss (Labaratory of Translational Research, Bethesda) provided mARH1 cDNA.

Michael O. Hottiger, Jeannette Abplanalp and Stephan Christen provided valuable editorial assistance and critical input during the writing.

Last but not least I want to thank the whole Hottiger group for giving me assistance and for making me laugh even during hard times. I also want to thank my family including Edgar and Benni for supporting me in everything I do and for their patience.

11 Curriculum vitae

Personal Information

Name	**Roentgen**
Given Name	**Anne Marie**
Date of Birth	**August 2nd, 1989**
Place of Birth	**Zurich, Switzerland**
Nationality	**Swiss, German**
Place of origin	**Thalwil ZH**

Education

1996 - 2002	Elementary school, Thalwil, Switzerland
2002 - 2004	Junior high school, Thalwil, Switzerland
2004 - 2008	High school, Enge, Zürich, Switzerland
Sept. 2008	Graduation from high school, focus on Modern Languages
2009 – 2010	Pharmaceutical Science, ETH Zurich, Switzerland
2010 – 2016	Veterinary Medicine, University of Zurich, Switzerland
30th Jan. 2017	Graduation from veterinary school, University of Zurich, Switzerland

Professional Activities

2008	Data evaluation assistant, Heptagon™, 8803 Rüschlikon, Switzerland

Research

Jan. 2014 – Aug. 2015	Master thesis, University of Zurich, Switzerland: "Volumetrische und morphologische Untersuchung lumbosakraler Bandscheiben anhand von MRT- und Röntgen-Studien" Supervision: PD Dr. med. vet. Dipl. ECVN, Frank Steffen, Department for Small Animal Surgery
Jan. 2015 – Jan. 2016	Doctor thesis, University of Zurich, Switzerland: "ARH1 regulates LPS-induced *iNOS* expression" Supervision: Prof. Dr. Dr. Michael O. Hottiger, Department of Molecular Mechanisms of Disease